Journal of Paleontology

www.cambridge.org/jpa

Articles

Cite this article: Anderson E.P., Rosbach S.A., Pulsipher M.A., Mikulic D., and Schiffbauer J.D. 2025. The 'butterfly animal,' *Papiliomaris kluessendorfae* n. gen. n. sp.: An enigmatic bivalved arthropod of the Waukesha biota. *Journal of Paleontology*, 1–17
https://doi.org/10.1017/jpa.2025.10102

Received: 09 September 2024
Revised: 07 February 2025
Accepted: 10 March 2025

Corresponding author:
James D. Schiffbauer;
Email: schiffbauerj@missouri.edu

Handling Editor:
Olev Vinn

The 'butterfly animal,' *Papiliomaris kluessendorfae* n. gen. n. sp.: An enigmatic bivalved arthropod of the Waukesha biota

Evan P. Anderson[1], Stephanie A. Rosbach[2], Mikaela A. Pulsipher[3], Donald Mikulic[4] and James D. Schiffbauer[2,5]

[1]Department of Earth Systems and Society, Pima Community College, Tucson, Arizona 85709, USA
[2]Department of Geological Sciences, University of Missouri, Columbia, Missouri 65211, USA
[3]Delaware North, Sequoia National Park, CA 93262
[4]Weis Earth Science Museum, University of Wisconsin—Oshkosh, Fox Cities Campus, Menasha Wisconsin 54952, USA
[5]X-ray Microanalysis Laboratory, Pima Community College, Columbia Missouri 65211, USA

Abstract

The phylogenetic relationships among arthropods remain contentious because morphological studies face challenges in resolving certain branches. Particularly difficult are relationships within and between the stem arthropods, owing largely to too few well-preserved fossil representatives. Additional fossil evidence, particularly from exceptional deposits like the Silurian Waukesha Lagerstätte in Wisconsin, helps to bolster our views on the evolutionary history of arthropods by providing well-preserved examples of novel taxa that could fit between early diverging stem-arthropod clades and modern euarthropods, thus building possible bridges between the two. Formed in karstification-induced troughs of the Manistique Formation paleoslope, the Waukesha Lagerstätte preserves a unique biota of organisms from the Telychian Age, mostly through secondary precipitation of francolite. Perhaps most well known from this deposit are the many peculiar and enigmatic arthropod taxa that could help resolve early arthropod cladistic relationships. We add to the growing body of work on the diversity, phylogeny, and taxonomic descriptions of the Waukesha biota by detailing a previously unnamed bivalved arthropod, informally called 'the butterfly animal' in past literature—which we here designate as *Papiliomaris kluessendorfae* n. gen. n. sp. We also conducted a Bayesian phylogenetic analysis that placed several recently described Waukesha taxa as basal members of the 'Mandibulate' clade within the Euarthropoda.

UUID: http://zoobank.org/c1d6f1dc-d35f-420c-aa57-2c8983f9779e

Non-technical Summary

The evolutionary relationships between arthropods are still debated because, in many cases, it is difficult to sort out connections based on physical traits alone. This is especially true when it comes to the relationships between early fossil arthropods and their modern descendants, mainly because there are not enough well-preserved fossils to study. However, discovering more fossils—especially from rare, well-preserved deposits like the Silurian Waukesha Lagerstätte in Wisconsin—can help us understand how arthropods evolved.

The Waukesha fossil deposit, which formed in ancient stagnant troughs, holds a unique collection of organisms from the Telychian Age of the Silurian Period, including many strange and enigmatic arthropods. In our study, we contribute to this research by describing a previously unnamed arthropod but one of the most charismatic of the deposit, formerly referred to as 'the butterfly animal,' which we here name *Papiliomaris kluessendorfae* n. gen. n. sp. in memoriam and honor of Dr. Joanne Kluessendorf, discoverer of the Waukesha Lagerstätte.

Introduction

The evolutionary history of arthropods, specifically the phylogenetic relationships between morphologically distinct clades, is still a hotly debated topic among invertebrate paleontologists and modern biologists (e.g., Scholtz and Edgecombe, 2006; Budd, 2008; Edgecombe, 2010; Ortega-Hernández, 2015; Giribet and Edgecombe, 2019). Their flexible body plan and morphological diversity create a complex and difficult to resolve phylogenetic tree. Extant Euarthropoda contains two established monophyletic groups: Mandibulata and Chelicerata. The confidence in monophyly of these two groups is in part owed to the availability of genetic analyses on extant taxa, which have also resolved placement of many additional clades within them (Regier et al., 2010; Rota-Stabelli et al., 2011; Giribet and Edgecombe, 2019). However, the topology of the

broader Euarthropoda (and, particularly the proposed Panarthropoda inclusive of the euarthropods, tardigrades, and onychophorans) presents difficulties, because these more expansive clades contain many fossil taxa classified as stem-group arthropods that do not fit within the established monophyletic clades of Euarthropoda. Although some of these fossil taxa can be coalesced into clades united by distinctive synapomorphies, (e.g., hymenocarines [Zhai et al., 2019] and fuxianhuiids [Aria et al., 2021]), it is common for fossil taxa to lack diagnostic features that would allow confident assignment, either authentically or due to taphonomic loss or bias (e.g., Aria et al., 2023). In addition to a lack of consistently defined morphological traits and too few well-preserved or well-described taxa being confounding in their own right, these uncertainties muddy the evolutionary relationships between extant Euarthropoda and the base of the euarthropod stem (Ortega-Hernández, 2015; Vannier et al., 2018; Yang et al., 2018; Giribet and Edgecombe, 2019), and result in conflicting hypotheses that plague this area of the arthropod phylogenetic tree (Giribet and Edgecombe, 2019).

To elucidate the phylogenetic relationships of early arthropods, many high-quality arthropod fossils across the Paleozoic have been (and continue to be) described in detail and added to the arthropod phylogenetic tree. Sourcing fossil material from deposits that preserve soft and chitinous tissues in great detail—Konservat Lagerstätten—has been paramount in providing enough morphological information to be useful in cladistic endeavors. Soft-bodied preservation of arthropods was relatively common in the Cambrian and Ordovician periods, with well-known fossil lagerstätten like the Burgess Shale (Briggs et al., 1994), Spence Shale (Robison and Babcock, 2011), Fezouata Formation (e.g., Van Roy and Briggs, 2011; Legg, 2016; Lustri et al., 2024), Beecher's Trilobite Bed (Farrell et al., 2011), Soom Shale (Gabbott et al., 2017), and Winneshiek Shale (e.g., Lamsdell et al., 2015a, b). By comparison, the Silurian has far fewer examples of exceptional arthropod preservation, and these lagerstätten are generally understudied, although notable examples include the Herefordshire Lagerstätte (Coalbrookdale Formation; e.g., Siveter et al., 2020) and Eramosa Lagerstätte (Lockport Group; e.g., Von Bitter et al., 2007) from the mid-Silurian Wenlock Epoch. However, the position of these lagerstätten in time leaves at least a ~10 Ma gap between those of the latest Ordovician and middle Silurian.

Primed to fill this void in arthropod evolutionary understanding, the Waukesha Lagerstätte of the Brandon Bridge Formation, Wisconsin, USA, was deposited in the earliest epoch of the Silurian, the Llandoverian, and preserved a diverse assemblage of soft-bodied fauna, including many well-preserved and enigmatic arthropods (Mikulic et al., 1985a, b; Wendruff et al., 2020a). Initial investigative efforts outlined the stratigraphy, sedimentology, and depositional history of this deposit (Mikulic et al., 1985a, b; Kluessendorf, 1990; Kluessendorf and Mikulic, 1996), but the pace of investigation on the fossils of this deposit was relatively slow until the mid-2010s. Recent works provide taphonomic and fossil descriptions of some of the numerous enigmatic arthropod fossils, including chelicerates (Moore et al., 2005; Wendruff et al., 2020a), basal mandibulates (Haug et al., 2014; Pulsipher et al., 2022), crustaceans (Jones et al., 2015a), myriapods (Wilson et al., 2004; Westberg, 2019), and an enigmatic arthropod with possible fuxianhuiid or cheloniellid affinities (Wendruff et al., 2020b; Anderson et al., 2021; Braddy and Dunlop, 2021; Van Roy et al., 2022). Despite the uptick in recent efforts, there are still many fossils left to be described, including two leperditicopid ostracod species, several trilobites, and two bivalved arthropods, among several others (Mikulic et al., 1985a; Jones and Tashman, 2016; Wendruff et al., 2020a; Gass and Braddy, 2023). This study adds to the growing body of work on the diversity of the Waukesha Lagerstätte by describing one of the unique bivalved arthropods from this pivotal deposit—an organism previously known as the 'butterfly animal' (Meyer and Gunderson, 1986).

Geologic setting

Initially described in 1985 (Mikulic et al., 1985b), the Waukesha Lagerstätte is a fossiliferous unit within the Brandon Bridge Formation, ranging in age from 438.5–433.4 Ma, upper Llandovery Epoch, Telychian Age (Fig. 1; Mikulic et al., 1985b; Kluessendorf and Mikulic, 1996; Kleffner et al., 2018). The Brandon Bridge Formation was deposited on the western side of the Michigan Basin and extends from northern Illinois into southern Wisconsin, pinching out against a paleoslope of the Silurian Manistique Formation in the Milwaukee area (Mikulic, 1977; Mikulic et al., 1985a, b; Kluessendorf, 1990; Kluessendorf and Mikulic, 1996). The Waukesha Lagerstätte is ~1 m thick and positioned ~2 m above the disconformity between the Manistique and Brandon Bridge formations (Kluessendorf and Mikulic, 1996). Most paleobiological studies, including this one, focus on samples from a 12 cm thick bed at the bottom of the Waukesha Lagerstätte collected from the Waukesha Lime and Stone Company quarry (43.03°N, 88.21°W) in Waukesha, Wisconsin, although the exposure yielding this bed is no longer accessible today (e.g., Moore et al., 2005; Haug et al., 2014; Jones et al., 2015a; Wendruff et al., 2020a, b; Anderson et al., 2021; Pulsipher et al., 2022). Samples from this unit are deposited in troughs in the Manistique Formation paleoslope that formed from karstification of the surface during a brief period of subaerial exposure. As sea level rose and the Brandon Bridge Formation began to be deposited, the troughs produced anoxic sediment traps in the shallow, poorly circulated peritidal environment that enabled preservation of the soft-bodied organisms now known as the Waukesha biota (Kluessendorf, 1990; Pulsipher et al., 2022). Particularly, the beds containing the Waukesha biota are found at the base of the paleoslope eroded into the Manistique Formation (Mikulic et al., 1985a; Kluessendorf, 1990; their 'cherty dolomite') where the paleoslope could have acted as a 'backstop' for circulation, maximizing the potential for stagnation and accumulation of soft-bodied debris in sediment traps (Supplementary Fig. 1).

Methods and materials

This study examines 11 undescribed arthropod fossils with similar morphologies from the Waukesha Lagerstätte. Six of these samples consist of part and counterpart (UWGM 2632a, b; 2633a, b; 2654a, b; 2655a, b; 2845 and 2719; 2882a, b), whereas the remaining five only consist of a singular part (UWGM 2631, 2856, 2862, 2983, 2985). All samples were borrowed from the University of Wisconsin Geology Museum (UWGM) for direct study, except UWGM 2719, which could only be photographed. The holotypes, paratypes, and additional material are permanently housed at UWGM.

Specimens were photographed with varying light angles to capture subtle details on the fossil surface using a Nikon D3300 digital camera attached to a Nikon SMZ1500 stereomicroscope. Digital video microscopy was also conducted using a Keyence VHX-7000. In Affinity Designer software (Serif Europe Ltd., 1987), morphological features were traced (using a Wacom Intuos Pro tablet interface) on aligned and stacked photographs. Morphological features observed in these images were examined to

https://doi.org/10.1017/jpa.2025.10102 Published online by Cambridge University Press

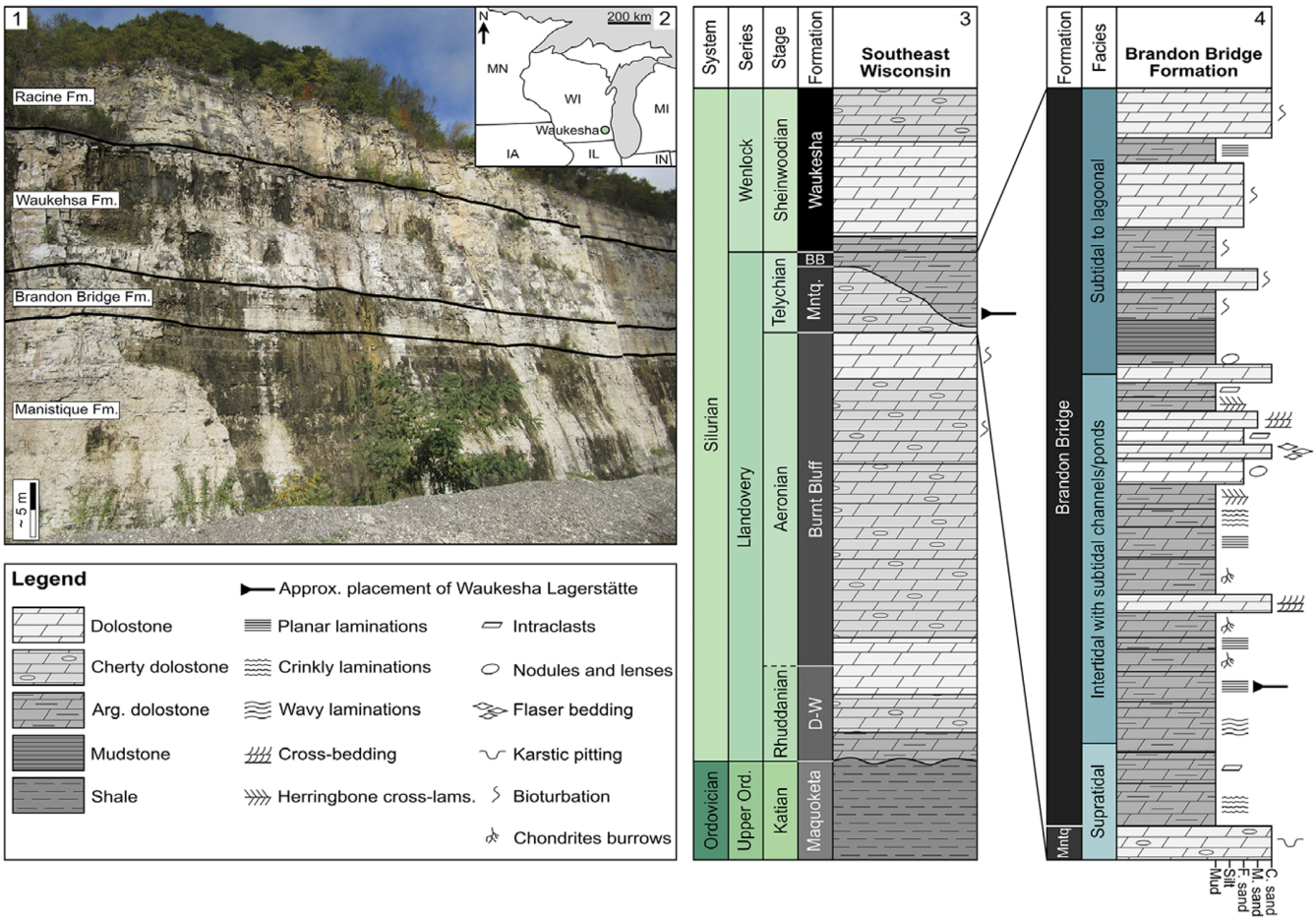

Figure 1. Geological setting of the Waukesha Lagerstätte, modified after Pulsipher et al. (2022). (**1**) Field photograph from the Waukesha Lime and Stone Company quarry. The Brandon Bridge Formation is exposed well above the quarry floor, and the quarry wall is ~45 m tall. Vertical foreshortening makes establishing a scale difficult, thus, the included scalebar is only a valid approximation in the vicinity of the Brandon Bridge Formation outcrop. (**2**) Inset map showing approximate location of Waukesha, Wisconsin. (**3**) Uppermost Ordovician and lower Silurian stratigraphic column of southeastern Wisconsin (after Wendruff et al., 2020a). (**4**) Idealized stratigraphic column of the Brandon Bridge Formation (after Kluessendorf, 1990) showing the overall deepening-upward facies package. In both (**3**) and (**4**), the Brandon Bridge Formation has a maximum thickness of 8 m; the horizon bearing the Waukesha Lagerstätte is located ~2 m above the underlying paleoslope and is denoted by the inverted black arrow. Arg. = argillaceous; BB = Brandon Bridge Formation; C. sand = coarse sand; D-W = Drummond-Wilhelmi Formation; F. sand = fine sand; Fm. = Formation; lams. = laminations; M. sand = medium sand; Mntq = Manistique Formation; Ord. = Ordovician.

determine their most plausible identity within a generalized arthropod morphological framework.

Phylogenetic analyses. Morphological characters of this taxon were coded into the Aria (2020) arthropod character matrix, composed of 268 morphological characters and a total of 110 taxa, both extant and extinct, including the addition of *Parioscorpio* Wendruff et al., 2020b, *Acheronauta* Pulsifer et al., 2022, *Captopodus* Kühl and Rust, 2012, and the Thylacocephala, as amended by Pulsipher et al. (2022). The full character matrix is available in the Supplementary Online Materials (SOM). The characters in the matrix primarily describe the external morphology of the included organisms, with large numbers of characters dedicated to the tagmata, segmentation, limb structure (particularly that of the head limbs), and other exoskeletal adornments. But many characters also describe internal organs, specifically the brain and digestive systems (Aria, 2020). As examination of the material and character coding proceeded, it became apparent that the morphology of the butterfly animal and its quality of preservation only sometimes allowed for an unambiguous interpretation. For several characters, multiple equally plausible judgments existed. Rather than arbitrarily deciding upon one hypothesis, five alternate hypotheses with decreasing levels of uncertainty across three sets of characters were coded into the matrix and tested individually. These hypotheses progressed from the most conservative character state interpretation, allowing for the most uncertainty, to two alternative hypotheses with the most defined character states (Table 1). Characters that differed between these hypotheses concern whether the

Table 1. *Papiliomaris* n. gen. character matrix hypotheses; all five hypotheses and coding of their relevant characters

	Character states		
Hypotheses	Carapace	2nd head appendage	Trunk limbs
Papilio-C	Uncertain	Uncertain	Uncertain
Papilio-BiCar	Bivalved	Uncertain	Biramous
Papilio-UniCar			Uniramous
Papilio-BiCar2		Reduced endopod	Biramous
Papilio-UniCar2			Uniramous

https://doi.org/10.1017/jpa.2025.10102 Published online by Cambridge University Press

anterior ornament was coded as a carapace (characters 38–48, 55–57); how the structure of the second head appendage, specifically the endopod, was coded (characters 131, 133–138); and interpretation of the trunk limbs (characters 230, 231, 239, 243). The first hypothesis, Papilio-C, served as a control, where all three relevant structures were coded as uncertain. Hypotheses Papilio-BiCar and Papilio-UniCar, kept uncertainty in the second head appendage description, but coded the bivalved carapace condition, and the trunk limbs either as rod-like biramous or paddle-like uniramous interpretations, respectively. The final two hypotheses, Papilio-BiCar2 and Papilio-UniCar2, had no uncertainty coded into the relevant characters. In these hypotheses, the bivalved carapace and two sets of trunk-limb character states were retained from the previous two hypotheses with similar names, but the second head appendage was defined as an endopod. All other characters were held constant between hypotheses.

We determined the phylogenetic placement of each hypothesis with Bayesian phylogenetic analyses in MrBayes v. 3.2.7 software (Ronquist et al., 2012). Software settings were retained between runs to ensure fair comparisons among final trees. For each MrBayes run, we used a gamma model with four runs of 2.5 million generations each and a 20% burn-in. Additionally, the analysis retained the molecular-data backbone for the tree, as designated and used by Aria (2020), to maintain crown-group arthropod topologies. Finally, tree output files from MrBayes were converted into images with FigTree v. 1.4.4 (Rambaut, 2018).

Scanning electron microscopy. We assessed fossil preservation by analyzing samples with a Zeiss Sigma 500 variable pressure scanning electron microscope (SEM) housed at the University of Missouri X-ray Microanalysis Laboratory. Sample surfaces were analyzed with a low-vacuum-specific cascade current secondary electron (SE) detector (for topography) and a five-segment, high-definition backscattered electron (BSE) detector (for composition). Operating conditions were as follows: 20 keV beam accelerating voltage, 40 nA current, a 60-µm aperture size, and vacuum chamber pressure was held at 20 Pa (chamber atmosphere = 99.999% nitrogen). While imaging, a working distance of 16 mm ± 1 mm was maintained with variation owing to small-scale changes in sample thickness and topography. Mosaics of SE and BSE images were compiled in the ATLAS microscopy workflow (Fibics Inc.) in three mixtures: 100% SE, 50% split between SE and BSE, and 100% BSE.

To investigate the composition of the samples further, we collected elemental data on sections of each sample with dual co-planar Bruker XFlash energy dispersive X-ray spectrometers (EDS). All operating conditions, except aperture size, were retained from the previous SEM imaging; aperture size was increased to 120 µm to increase X-ray signal, achieving a total count rate of 150 kilocounts/sec with both detectors in tandem.

Repository and institutional abbreviation. All specimens are reposited at the University of Wisconsin Geology Museum (UWGM), Madison.

Systematic Paleontology

Phylum **Euarthropoda** Lankester, 1904
Genus ***Papiliomaris*** new genus

Type species. Papiliomaris kluessendorfae n. gen. n. sp., by monotypy.

Diagnosis. As for type species by monotypy.

Etymology. Papilio: L., butterfly, and *maris*, genitive form of *mare*, L., sea; meaning butterfly of the sea or sea butterfly, paying homage to classic literature on the Waukesha fossils that nicknamed this organism 'the butterfly animal', owing to its butterfly-like appearance.

Occurrence. Waukesha Lagerstätte, Brandon Bridge Formation, Waukesha Lime and Stone Company quarry, Waukesha, Wisconsin, USA.

Remarks. As for species.

Papiliomaris kluessendorfae new genus new species
Figures 2–5

Type specimens. Holotype, UWGM 2655, part and counterpart, Telychian Stage of the Llandovery Epoch, Silurian, Waukesha Lagerstätte, Brandon Bridge Formation, Waukesha, Wisconsin, USA. Paratypes, UWGM 2633, part and counterpart, and 2654, part and counterpart, sam locality as holotype.

Diagnosis. Bivalved arthropod with two tagmata. Near circular to ellipsoid valves attached anteriorly in vicinity of fourth or fifth cephalic somite. Remaining hinge disconnected from cephalon. Valves covering posterior three to four head appendages. Uniramous antennae on second and third somites. Robust, annulated, coarsely setose primary antennae extending anterodistally, can recurve posteriorly. Second antenna on third somite delicate and elongate with closely set rows of setae. Posterior three cephalic limbs elongate and somewhat flexible with at least two rows of filamentous setae. The third of these elongate appendages, found on the sixth somite, noticeably smaller compared to two preceding it. Short trunk, 10−13 segments decreasing in width posteriorly. Raised central ridge along dorsal tergites. Small pleurae extending posterodistally from each tergite. Homogenous bifurcated rod-like or uniramous paddle trunk limbs. Trunk terminating with reduced telson.

Description. Papiliomaris kluessendorfae n. gen. n. sp. has two tagmata: a six-somite cephalon with a bivalved carapace and a trunk comprised of 10−13 somites (Fig. 2.1–2.3). Intact samples range in length from 11.5–20.8 mm, with a mean ± 1 standard deviation (SD) of 15.2 ± 0.6 mm; width ranging from 8.8–17.4 mm, with a mean ± 1 SD of 12.3 ± 0.6 mm. The first (ocular) segment has no preserved specialized structures (Fig. 2.3), including eyes, whereas the remaining five are limb-bearing (Figs. 2.3, 3.8). The second and third head segments each bear a single pair of antennae (Fig. 3.1–3.3). The primary antennae are robust, annulated, and bear large, thick, spiny setae (Figs. 3.2, 5.6). Secondary antennae are preserved in two specimens—UWGM 2633 (Fig. 3.3) and 2845 (Fig. 4.2, 4.3)—and are moderately long with fine, closely-spaced setae, perhaps organized in a single row; the holotype indicates the original presence of these structures by limb bases seen adjacent to the third head segment ('2nd Antenna Base?'; Fig. 2.2, 2.3, 2.5). The nature of the ramus is unknown for the second antenna.

The remaining three cephalic somites have a single pair of simple, elongate limbs with no clear annulations that bear multiple rows (at least two) of long, filamentous setae (Figs. 2.3, 3.5–3.8). The insertion points of these limbs can be visible on the body (Fig. 2.4, 2.5), whereas the rami are putatively preserved in a few specimens, either as gentle impressions (Fig. 2.2–2.5) or more

https://doi.org/10.1017/jpa.2025.10102 Published online by Cambridge University Press

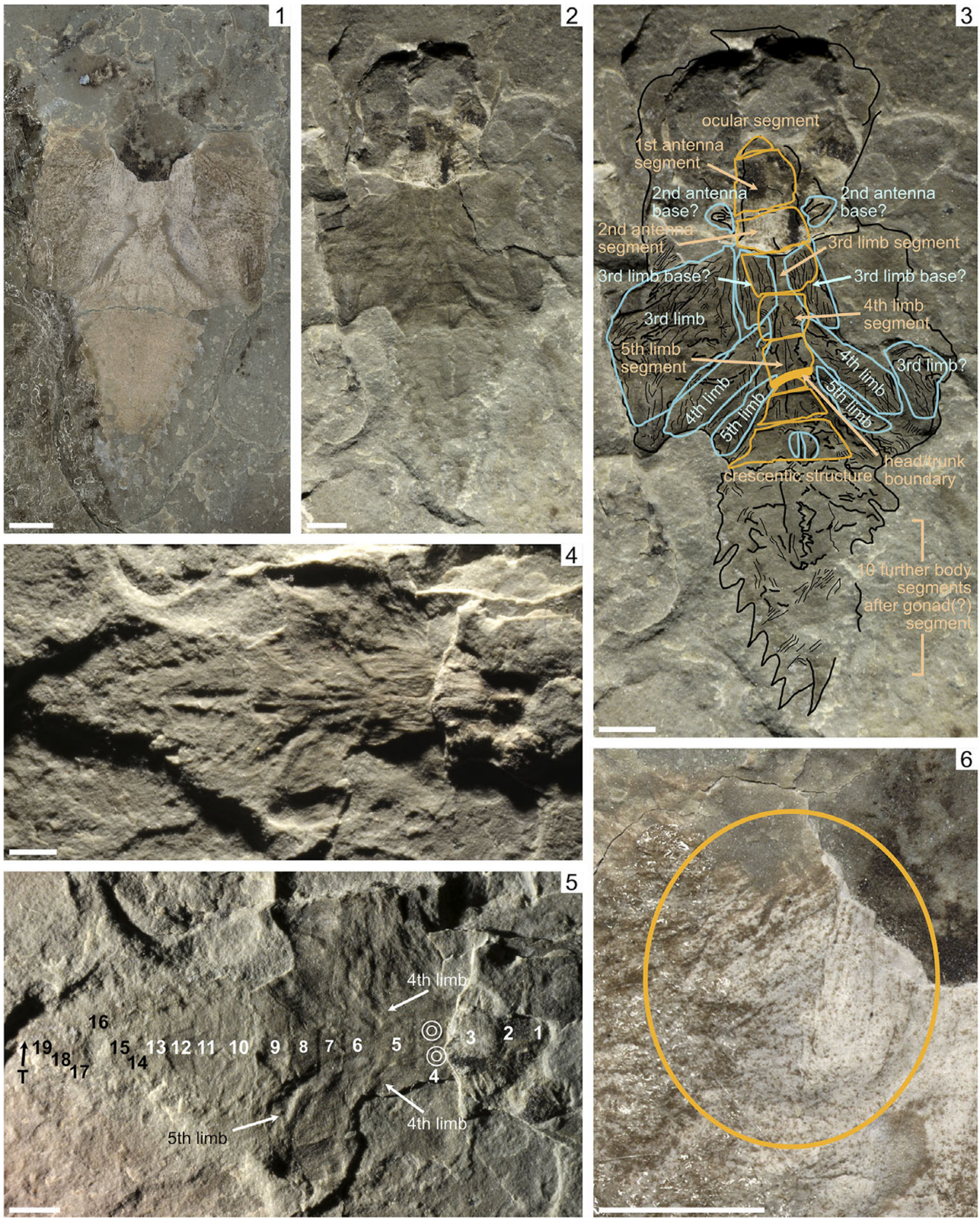

Figure 2. Holotype UWGM 2655 (part and counterpart) of *Papiliomaris kluessendorfae* n. gen. n. sp. (**1**) Normal lighting with glare reduction showing part. (**2**) Normal lighting of counterpart. (**3**) Interpretive traces of counterpart, based on photographs taken with multiple lighting angles. Major fossil and topographic features in heavy black lines, finer fossil features in light black lines, areas of the fossil associated with limbs or limb features outlined and labeled in light blue, and areas of the fossil associated with segments outlined and labeled in orange. (**4**) Photograph of counterpart with raking light from the north, highlighting features of the limbs and limb bases. The limb insertions and limbs highlighted in (**5**) are visible in (**4**), as well. (**5**) Photograph of counterpart with raking light from the west, highlighting features of the limbs and segment divisions. The 'bullseyes' highlight potential limb insertions on somite 4, which bears the first postantennal limb. Somites are labeled sequentially, those in white font are more confidently identified. Numbers can be staggered due to spacing, although somite 16 is not well preserved. (**6**) Detail view of part with an ellipse highlighting the preserved axis of bifurcating setae, indicating the presence of limb 3. Scale bars = 2 mm.

https://doi.org/10.1017/jpa.2025.10102 Published online by Cambridge University Press

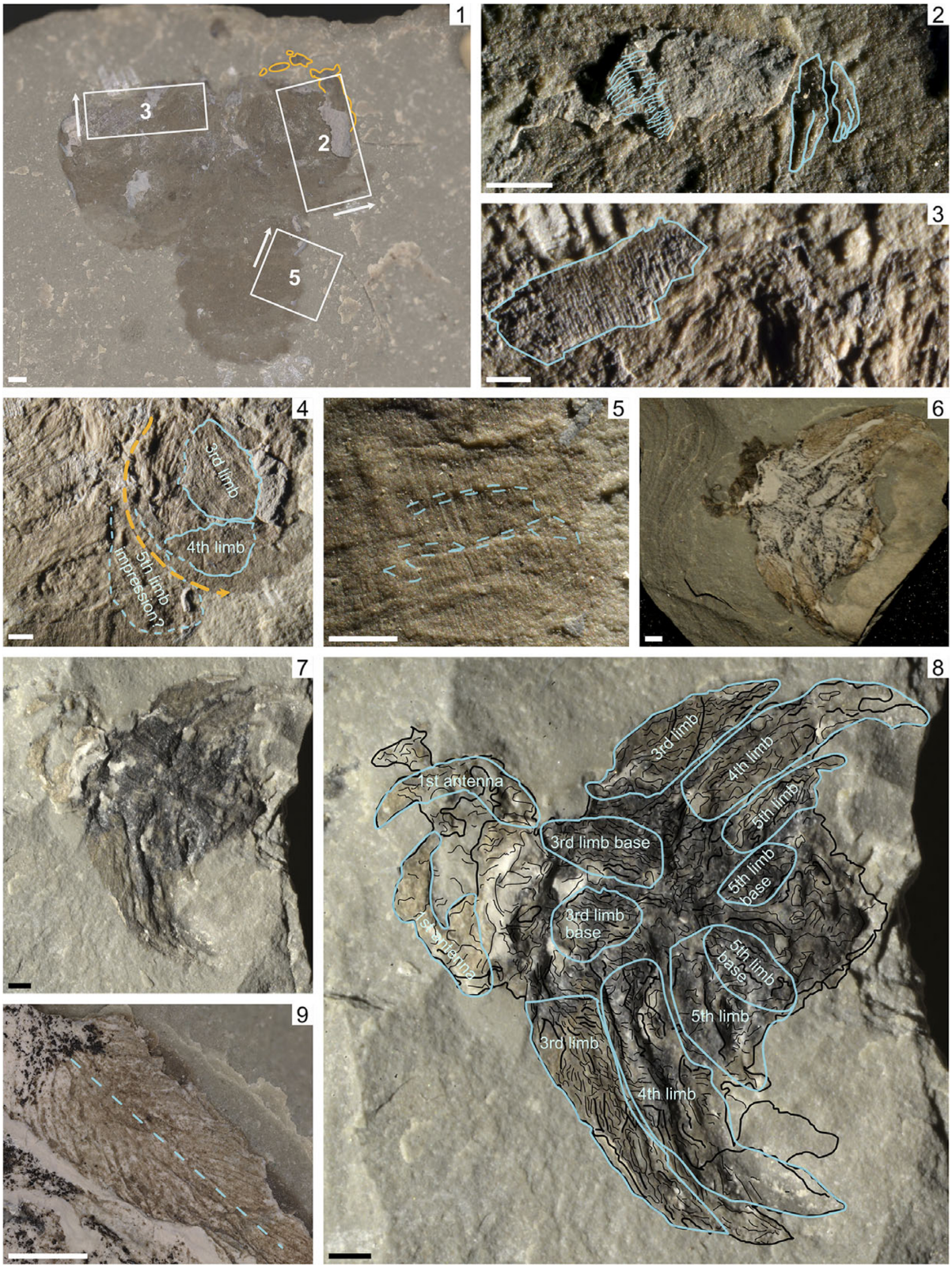

Figure 3. Paratypes of *Papiliomaris kluessendorfae* n. gen. n. sp. (**1–5**) UWGM 2633, a specimen (part and counterpart, the latter not figured) with good preservation of the head limbs and the anterior trunk: (**1**) Photograph of part with normal lighting; labeled boxes indicate areas shown in (**2**), (**3**), and (**5**). Orange-outlined region shows fragmental preservation of the first antenna medial to the well-preserved portion shown in (**3**). (**2**) Distal first antenna; the last two segments with large spiny setae are traced on the right, whereas a sampling of potential cross-cutting setulae are traced on the left. (**3**) An unusual second antenna preserved in francolite. The approximate extent of second antenna preservation is traced; setae from subsequent head limbs crisscross lower in the photograph. (**4**) Right side of the specimen under raking light from the west showing the medial edge of the right carapace valve, outlined in dashed orange. Partially preserved third and fourth limbs (dashed blue lines indicate that the limbs likely continued but have not been preserved) and the impression of the fifth limb allow for the placement of the carapace with respect to the head segments to be deduced. (**5**) Potential trunk limbs preserved as molds, which can either form paddles or two curling rami that meet distally. One potential limb is traced, and there are additional limbs preserved to the anterior and, particularly, the posterior. (**6–9**) UWGM 2654 (part and counterpart) of *Papiliomaris kluessendorfae* n. gen. n. sp. Specimen does not preserve a carapace yet shows anomalously high preservation quality in francolite and in a carbon film. (**6**) Normal light photograph of counterpart, exhibiting the extensively phosphatized axial body and limbs 3–5. (**7**) Photograph of part with a high angle raking light from the northwest. (**8**) Enlargement of (**7**) overlain by interpretive traces based on viewing the specimen from multiple lighting angles. Major fossil features in heavy black lines, finer fossil features in light black lines, with limbs and limb features outlined in light blue. Compare to the morphologies seen in (**6**). (**9**) Detail of the third limb on the counterpart, which shows the bifurcating setae of the limb in francolite. The dashed line indicates the interpreted position of the limb's central ramus. Scale bars = 1 mm.

https://doi.org/10.1017/jpa.2025.10102 Published online by Cambridge University Press

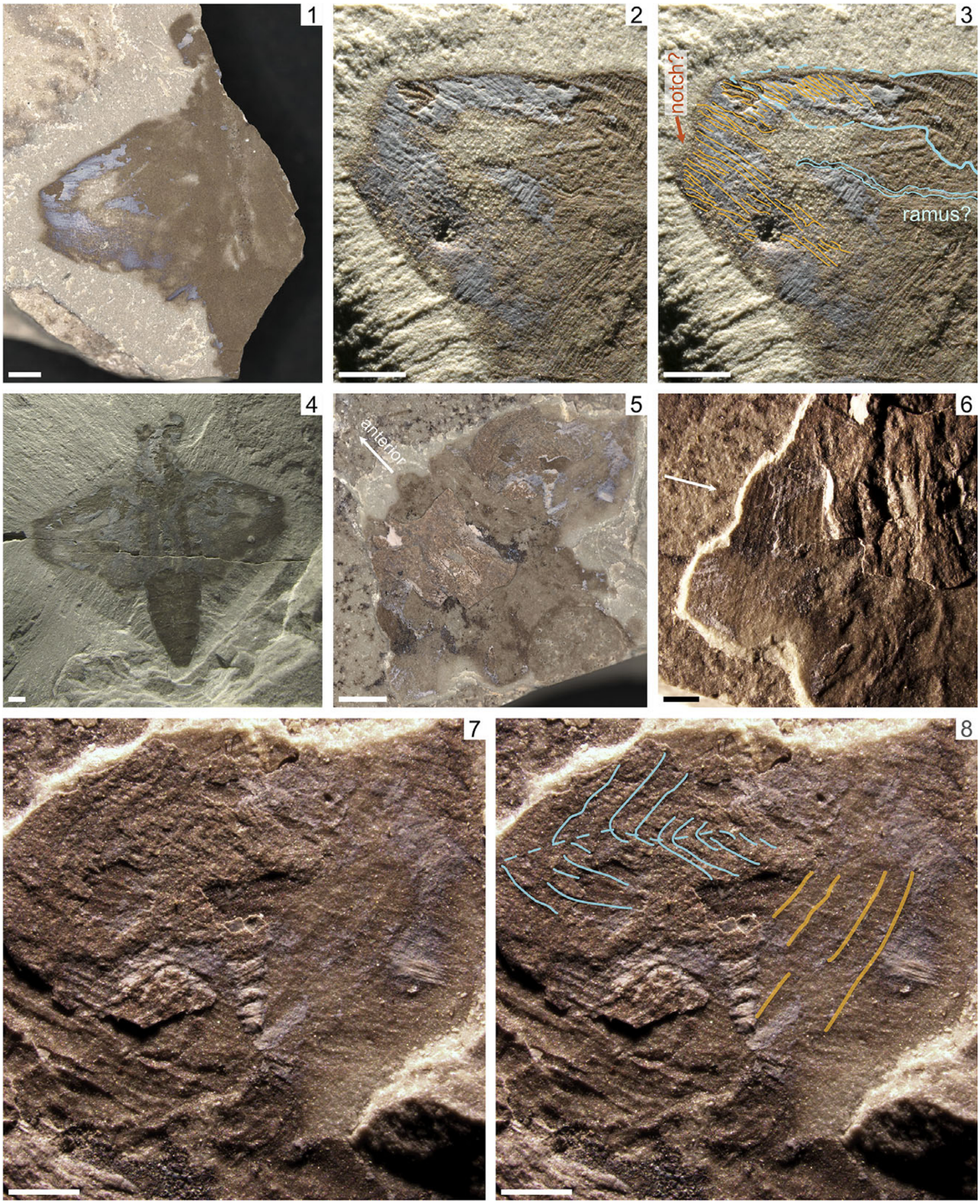

Figure 4. Selected well-preserved specimens of *Papiliomaris kluessendorfae* n. gen. n. sp. (**1–4**) UWGM 2845 and 2719, part and counterpart, a carapace-bearing specimen with limited phosphatization but extensive moldic limb and carapace details when viewed under raking light. (**1**) Photograph of UWGM 2845 under normal light; little detail is revealed. (**2, 3**) Photograph of UWGM 2845 without and with interpretive tracing, respectively. The upper light blue outline traces the extent of the second antenna (dashed line indicates increased uncertainty, its base is not apparent), whereas the lower light blue outline labeled 'ramus?' traces a possible decayed head limb. The orange arrow labeled 'notch?' indicates a sharp angle on the carapace also observed in UWGM 2862 (Fig. 5.9). The traced orange grooves highlight obliquely transverse ribs on the carapace: their spacing is generally wider than the setae, and they can be traced straight across broad expanses of the carapace. (**4**) Photograph of UWGM 2719; this is the 'bizarre arthropod' first featured by Mikulic et al. (1985a, b). (**5–8**) UWGM 2631, a partial specimen that preserves numerous details in francolite and as a mold. (**5**) Photograph of specimen under normal light; francolite is mostly hidden beneath a carbon film, with some darker kerogenous regions present. Arrow indicates the front end of the animal. (**6**) Detail photograph with raking light from the west of the incomplete left carapace of the specimen. The longitudinal ribs are strongly seen, with arrow pointing perpendicularly toward them. (**7, 8**) Detail photograph with raking light from the north of the right half of the specimen, showing bifurcating setae of one of the head limbs highlighted in light blue, a dashed line indicating the inferred position of the setae's underlying ramus, and broad, gentle, obliquely transverse ribbing highlighted in orange (highlights in **8**). Stronger longitudinal ribs crisscross the transverse ones. Scale bars = 2 mm (**1**–**5**); 1 mm (**6–8**).

https://doi.org/10.1017/jpa.2025.10102 Published online by Cambridge University Press

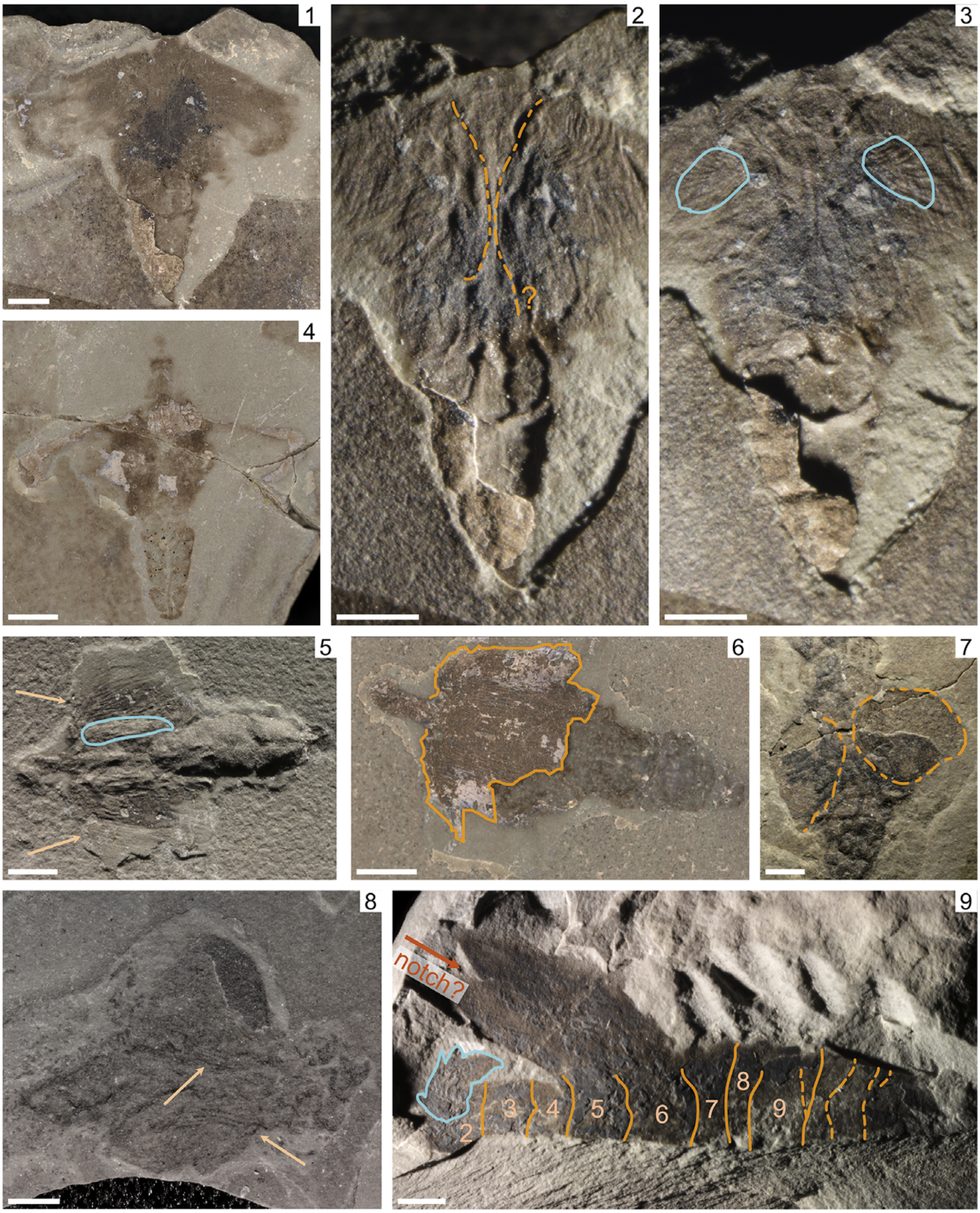

Figure 5. A selection of specimens of *Papiliomaris kluessendorfae* n. gen. n. sp. with little to no limb preservation, highlighting the shape of the carapace. (**1–3**) UWGM 2985, which has a well-preserved carapace and poorly preserved bases of some of the head limbs. (**1**) Photograph taken under normal light; its carapace has been anteriorly displaced and rotated, giving it a 'clothes-hanger' appearance. (**2**) Photograph of the specimen's axis under raking light from the east, showing the preserved medial edges of the left and right carapace valves in dashed orange. '?' indicates the uncertainty in the posteromedial shape of the right valve. (**3**) Photograph of the specimen's carapace under raking light from the south, rotated 90° counterclockwise compared to (**1**) and (**2**), showing the poorly preserved bases of head appendage 3. Compared to (**2**), note that appendage 3, and thus segment 4, lies just anterior to axialmost portion of the carapace valves. (**4**) Photograph of UWGM 2983 under normal light; its carapace valves have been rotated to appear much thinner longitudinally than in other specimens. It, too, has a clothes hanger-like appearance. (**5, 6**) Photographs of UWGM 2882 part and counterpart, respectively, showing longitudinal ribbing on the carapace valves. (**5**) Part under raking light from the north, highlighting the trunk preserved in thick, three-dimensional phosphate, and the carapace ribs (arrows)

(*Continued*)

https://doi.org/10.1017/jpa.2025.10102 Published online by Cambridge University Press

directly (Fig. 4.2, 4.3). More frequently, their position can be inferred through the presence of bifurcating setae (Figs. 2.6, 3.9, 4.7, 4.8). The relative size of these appendages can vary between specimens. In the holotype, limb three is somewhat longer and covers a much broader area than limbs four or five (Fig. 2.3), and in other specimens, the base of the third limb can appear robust even when the appendages are otherwise poorly preserved (compare Fig. 2.3 and 5.3). Yet, in paratype UWGM 2654, which has the best-preserved limbs of any specimen, it is the fourth limb that is the longest and covers a slightly wider area with its setae (Fig 3.6, 3.8). However, the fifth head appendage is always the smallest of the three, one-third the size of the larger of limbs three or four (Figs. 2.3, 3.8). Accounting for size variation, head appendages three through five are otherwise self-similar.

The attachment point of the bivalved carapace is not directly observed, but based on the closest, they are preserved to the axis, they likely attach in the vicinity of the posterior fourth cephalic segment, or even the anterior of the fifth (Figs. 3.4, 5.2–5.4, 5.7). The hinge of the carapace is otherwise liberated from the cephalon of the organism, allowing the valves to lift off the dorsal side (Fig. 5.1–5.4, 5.9). Each valve of the organism is rounded and somewhat longer than wide (i.e., widest transversely with respect to the orientation of the main body), covering the head appendages two to five or three to five and their setae with minimal to no overlap of the trunk segments (Figs. 3.4, 4.1–4.5, 5.2, 5.3, 5.5, 5.7, 5.8). Several specimens have a 'notch' in the distal end of the valve (Figs. 4.2, 4.3, 5.9) that might or might not represent a taphonomic artifact. If it is authentic, the lack of preserved posterior head limbs could explain why the notch appears much more distinct in UWGM 2862 (Fig. 5.9) compared to 2845 (Fig. 4.2, 4.3). Ornamentation of the carapace is difficult to determine. Prominent longitudinal ribs appear on some specimens and seem superimposed on other features of the head segments and limbs (Fig. 5.5–5.8). In some cases, these ribs have a wrinkled appearance (e.g., Fig. 5.2, 5.3) Yet, on others, obliquely transverse ribs can be seen on the carapace, also superimposing on other features of the head and head limbs (Fig. 4.2, 4.3). In UWGM 2631, both faint transverse ribs and stronger longitudinal ribs are seen (Fig. 4.6–4.8).

The trunk of *Papiliomaris kluessendorfae* n. gen. n. sp. contains 10–13 somites and a raised central ridge along the dorsal tergites (Fig. 2.3–2.5). It is not certain whether the variation in somite number is taphonomic, ontogenetic, or due to population variation, because only the holotype preserves the telson (Fig. 2.5). The first three anterior segments taper toward the cephalon (Fig. 2.3). However, whether this is inherent to the morphology or a preservational by-product of the overlying carapace and head limbs four and five covering portions of the anterior trunk segments is unclear (compare to Fig. 5.9). On a few specimens, there are paired axial crescentic structures on the anterior trunk, but they are only clearly preserved on the holotype on trunk segment 3 or somite 9 (Fig. 2.3–2.5). Given their rarity, it is difficult to say what these represent. The fourth and fifth trunk segments, found immediately posterior to the crescentic structures as somites 10 and 11 (Fig. 2.3, 2.5) attain the maximum trunk width, and the remaining segments taper toward a short telson on the posterior terminus. Each trunk segment has short pleurae that extend posterodistally (Figs. 2.3–2.5, 5.9). Trunk limbs are poorly preserved but show no indication of differentiation across the trunk. The appendages are either bifurcated rod-like limbs that curl toward one another laterally, or uniramous paddle limbs, which in either case can bear fine setae that cover the limbs (Fig. 3.5).

Etymology. The species epithet *kluessendorfae* is established in honor and memoriam of Joanne Kluessendorf, whose contributions were paramount to the discovery, description, and understanding of the sedimentology and paleontology of the Waukesha Lagerstätte and Brandon Bridge Formation.

Additional materials. Nine additional specimens, Telychian Stage of the Llandovery Epoch, Silurian, Waukesha Lagerstätte, Brandon Bridge Formation, Waukesha, Wisconsin, USA: UWGM 2631, 2632 a+b, 2719 and 2845 (part and counterpart), 2856, 2862, 2882a+b, 2983, 2985.

Remarks. Variations in the appearance of *Papiliomaris kluessendorfae* n. gen. n. sp. result from different preservational positions or compressional orientations and the extent of carapace and limb preservation. There is only one possible example of lateral compression, which resulted in a clear view of the tergite pleurae and partial preservation of some of the head appendages (Fig. 5.9). Dorsoventral compression is far more common but also varies in appearance depending on the position of the carapace. The carapace hinge being completely detached along its length (excepting the anteromedial edge) allowed it to lift during biostratinomy and burial. This process created a range of visible morphologies with two endpoints: one with the carapace directly overlying the head limbs, directed posterolaterally, and the other with it completely lifted and partially rotated, so that it would be compressed anteroposteriorly. The prior endmember preserves the most details in head appendages three to five, and sometimes head appendage two as well, lending a general protective effect of the carapace on limb detail preservation, and has an overall winged appearance as suggested by the generic name, *Papiliomaris* n. gen. (Figs. 2, 4.1, 4.4). When the carapace is lifted and rotated, the head appendages retain few details, and the valves are compressed to ellipsoids that extend laterally, giving a clothes hanger-like outline to the anterior body (Fig. 5.1–5.4). It is not impossible for in-place carapace valves to preserve the limbs poorly, as well (Fig. 5.5–5.8). Paratype UWGM

Figure 5. (Continued)
that imprint on both the thin, distal regions of the carapace, and the moldic axial regions without interruptions. Elongate depressions on either side of the axis (right one outlined in blue) compare favorably in position to the '3rd limb base' seen in Figure 2.3 and other specimens. It is likely the same structure here, despite the fact that no limbs are directly preserved in this specimen. (**6**) Counterpart under normal light; the axial region of the head segments is preserved with relatively thick francolite (traced in orange), presumably reflecting the preservation of visceral tissues, morphological details of which have since been largely lost. (**7, 8**) UWGM 2632a, b, a fairly poorly preserved specimen with evidence of a carapace, trunk segmentation, and substantial keroginization-encrusted phosphatization. (**7**) Photograph of UWGM 2632a under lightly raking light from the north, showing the carapace valves, highlighted in dashed orange. The lateral valve margin on the right could be a preservational artifact. (**8**) Photograph of UWGM 2632b under lightly raking light from the east, rotated 90° compared to the part in (**7**). The impressions of ribs on the carapace can be seen lateral to the specimen axis; the best areas are indicated by arrows. (**9**) Photograph of UWGM 2862 under low angle raking light from the north. An unusual and incompletely preserved specimen, it might show lateral preservation, or the left half might simply have broken off. The carapace shows a distinct, angled terminus of dubious significance, resembling the notch also seen in UWGM 2845, and wavy grooves on the anterior end could be a fragmentally preserved first antenna (traced in light blue). Orange numbers are putative somite numbers, based on the presence of lineations, highlighted in orange, which appear to be segment boundaries. The ocular segment is not distinguishable, and the segment boundaries become more questionable posteriorly, reflected by the dashed highlights. Scale bars = 2 mm.

https://doi.org/10.1017/jpa.2025.10102 Published online by Cambridge University Press

2654 is the singular exception to this pattern: it has no evident carapace preservation but retains well-preserved limbs that could be a result of high phosphate levels near this sample that made the carapace protection unnecessary (Fig. 3.6, 3.7). This visual variability complicated previous efforts to describe this fossil group.

Potential previous interpretations of these samples included a bivalved arthropod (e.g., Mikulic et al., 1985a) or a marrellomorph (e.g., Jones et al., 2015b). Although our assessment agrees with the bivalved arthropod characterization, several pivotal features prevent *P. kluessendorfae* n. gen. n. sp. from being placed within the marrellomorphs. For one, all known marrellomorphs have unique and ornate cephalic shields (e.g., *Marrella* Walcott, 1912; *Mimetaster* Gürich, 1932) or large, ovoid carapaces (e.g., *Vachonisia* Lehmann, 1956, *Skania* Walcott, 1931), whereas *P. kluessendorfae* n. gen. n. sp. has a bivalved and perhaps ribbed carapace with a short attachment to the body, and simple, ovoid valves (Figs. 3.4, 4.2, 4.3, 4.6– 4.8, 5; Rak et al., 2013; Moysiuk et al., 2022). As described above, the valves of *P. kluessendorfae* n. gen. n. sp. extend laterally like two hanger wings when the carapace lifts and rotates away from the cephalon (Fig. 5.1, 5.4). The appearance of the valves in this scenario is visually similar to the lateral spines on the cephalic shield of *Marrella splendens* Walcott, 1912. However, the flexibility of carapace valve orientation dependent on taphonomic circumstances shows that these are separate valves that fold along a hinge rather than one continuous shield structure (e.g., compare Figs. 3.1 and 5.1). Additionally, marrellomorphs characteristically have > 20 trunk somites, whereas *P. kluessendorfae* n. gen. n. sp. notably has a comparatively short trunk composed of relatively few segments. *Skania*, a marellomorph with few trunk somites, still bears a broad, body-encompassing carapace (Legg, 2015; Moysiuk et al., 2022), unlike that of *P. kluessendorfae* n. gen. n. sp. These two significant deviations in body plan exclude *P. kluessendorfae* n. gen. n. sp. from Marrellomorpha.

Papiliomaris kluessendorfae n. gen. n. sp. is not the first bivalved arthropod documented from the Waukesha Lagerstätte, either; previous works denote the presence of three other groups: leperditicopids, thylacocephalans, and phyllocarids (Mikulic et al., 1985a; Haug et al., 2014; Jones et al., 2015a). At least two species of leperditicopid ostracods are abundant on certain bedding surfaces (Mikulic et al., 1985a; Jones and Tashman, 2016); however, they have yet to be analyzed in detail or officially described. Differentiated from *P. kluessendorfae* n. gen. n. sp., the Leperditicopida Scott, 1961 represents an order of large ostracods with valves that enclose the entire organism. Leperditicopids are distinguished by a long straight hinge with varying degrees of unequal valves, a large abductor muscle scar, and poor segmentation (Scott, 1961; Berdan, 1984; Vannier et al., 2001; Abushik, 2015). Several features of *P. klussendorfae* n. gen. n. sp. are distinct from the leperditicopids and other ostracods, including the extension of the trunk outside of the carapace, valves that are symmetric in size and shape, an absence of muscle scars, and evident segmentation, particularly in the trunk.

Similar to the leperditicopids, the thylacocephalan genus *Thylacares* Haug et al., 2014 has been found in the Waukesha Lagerstätte and has a body fully enveloped in its bivalved carapace, with only the stalked eyes and raptorial appendages extending past the carapace margin (Haug et al., 2014). The extension of the trunk of *Papiliomaris klussendorfae* n. gen. n. sp. beyond the carapace, the apparent lack of a tight fit of the carapace around the body, and the lack of eyes and raptorial appendages exclude it from fitting within the definition of *Thylacares* or any other thylacocephalan. Additionally, the presence of 22 trunk segments in *Thylacares* (Haug et al., 2014) is nearly double the ~12 found in *P. kluessendorfae* n. gen. n. sp.

Three species of the phyllocarid genus *Ceratiocaris* M'Coy, 1849 are found in the Waukesha Lagerstätte (Jones et al., 2015a). *Ceratiocaris* is part of the extinct order of phyllocarids, Archaeostraca, which is partially defined by the presence of a hinged carapace and an elongated telson with two lateral furcal rami (Collette and Hagadorn, 2010). These latter two traits are notably lacking in *Papiliomaris kluessendorfae* n. gen. n. sp., which has a reduced telson and completely lacks furcal rami. Additionally, all phyllocarids exhibit three distinct tagmata, including eight limb-bearing thoracic or pereion somites and a seven-segmented pleon, whereas *P. kluessendorfae* n. gen. n. sp. only has an undifferentiated trunk behind its head (Collette and Hagadorn, 2010). The designation of *P. klussendorfae* n. gen. n. sp. as a new genus and species is thus a necessity given its distinction from these other documented bivalved arthropods.

Discussion

Phylogeny. The Bayesian phylogenetic analyses produced two different tree structures across all five morphological hypotheses. Hypotheses Papilio-C and Papilio-BiCar2 placed *Papiliomaris* n. gen. as sister to a clade containing *Acheronauta*, Thylacocephala, and *Captopodus*, which, collectively, is sister to Mandibulata. *Parioscorpio* placed as sister to the entirety of that clade (subsequently, this arrangement will be referred to as Tree A). The remaining three hypotheses, Papilio-UniCar, Papilio-UniCar2, and Papilio-BiCar, all shared a second resulting tree structure (hereafter referred to as Tree B). The topologies of Tree A and Tree B can be observed in Figure 6. Tree B places *Papiliomaris* n. gen. as sister to the clade containing the previously mentioned taxa (*Acheronauta*, Thylacocephala, and *Captopodus*) and the rest of Mandibulata, with *Parioscorpio* as sister to *Papiliomaris* n. gen. + Mandibulata, essentially distancing the relation of *Papiliomaris* n. gen. to *Acheronauta*, Thylacocephala, and *Captopodus* by one branching event (Tree B). There are a few small differences between the trees outside of the placement of *Papiliomaris* n. gen. In PapilioC, Papilio-UniCar2, and Papilio-BiCar, Megacheira is monophyletic, whereas in Papilio-BiCar2 and Papilio-UniCar, it is paraphyletic with *Haikoucaris* Chen, Waloszek, and Maas, 2004 + Leanchoiliidae as sister to the remaining Euarthropoda. Basal to the taxa shown in Figure 6, in Papilio-C, Papilio-BiCar2, and Papilio-UniCar2, Radiodonta is paraphyletic with *Hurdia* Walcott, 1912 + *Schinderhannes* Kühl, Briggs, and Rust, 2009 as sister to the Euarthropoda, whereas in Papilio-UniCar and Papilio-BiCar, it is monophyletic. Additionally, in Papilio-C, *Clypecaris* Hou, 1999 is sister to most of the Hymenocarina, whereas in other trees it is embedded higher in the clade, sister to *Canadaspis* Novozhilov, 1960 + [*Branchiocaris* Briggs, 1976 + *Tokummia* Aria and Caron, 2017]. Lastly, in Papilio-BiCar, *Burgessia* Walcott, 1912 is sister taxon to the remaining artiopods and Aglaspidida is sister to the included trilobites, whereas in other trees, these taxa switch places.

Other than this, the topologies of the five trees are identical, and common nodes have similar posterior probabilities (typically within 0.05), and any of the five starting hypotheses could be plausible interpretations for the morphology of *Papiliomaris* n. gen. (Table 1). However, given the lack of unambiguous details on the secondary antennae, we prioritized a more conservative interpretation. We therefore preferentially interpret *Papiliomaris* n. gen. to have a bivalved carapace, an uncertain description of the second head appendage, and either uniramous paddle-like or

https://doi.org/10.1017/jpa.2025.10102 Published online by Cambridge University Press

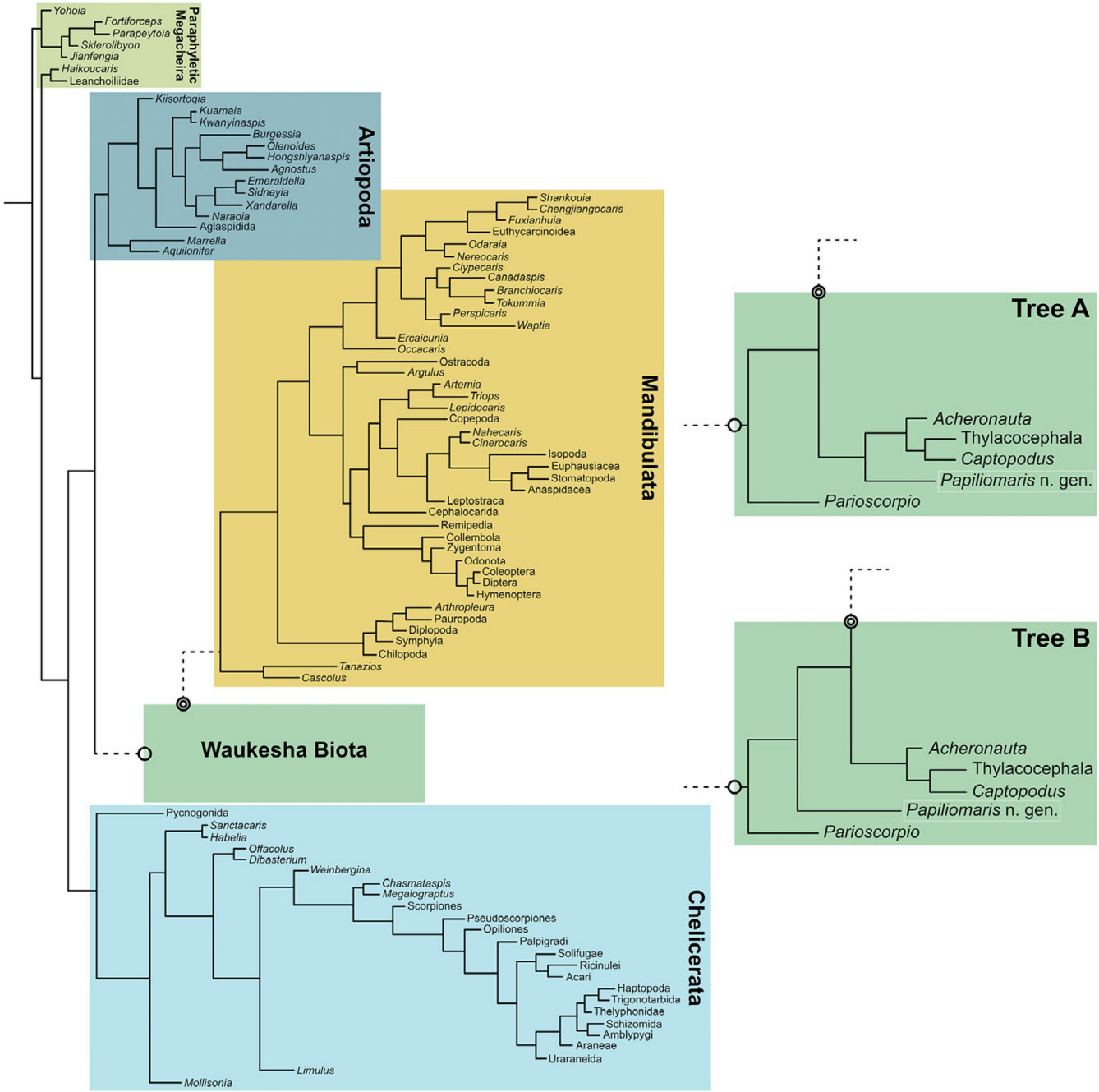

Figure 6. Phylogenetic trees resulting from MrBayes analyses. Waukesha topologies noted in 'Tree A' and 'Tree B' offsets. Taxa not otherwise mentioned in the text are: *Agnostus* Brongniart, 1822; *Aquilonifer* Briggs et al., 2016; *Argulus* Müller, 1785; *Artemia* Leach, 1819; *Arthropleura* Jordan in Jordan and von Meyer, 1854; *Chasmataspis* Caster and Brooks, 1956; *Chengjiangocaris* Hou and Bergström, 1991; *Cinerocaris* Briggs et al., 2003; *Emeraldella* Walcott, 1912; *Ercaicunia* Luo et al., 1999; *Fortiforceps* Hou and Bergström, 1997; *Fuxianhuia* Hou, 1987; *Habelia* Walcott, 1912; *Hongshiyanaspis* Zian and Lin in Zhang et al., 1980; *Jianfengia* Hou, 1987; *Kiisortoqia* Stein, 2010; *Kuamaia* Hou, 1987; *Kwanyinaspis* Zhang and Shu, 2005; *Lepidocaris* Scourfield, 1926; *Limulus* Müller, 1785; *Megalograptus* Miller, 1874; *Mollisonia* Walcott, 1912; *Nahecaris* Jaekel, 1921; *Naraoia* Walcott, 1912; *Nereocaris* Legg et al., 2012; *Occacaris* Hou, 1999; *Odaraia* Walcott, 1912; *Olenoides* Meek, 1877; *Parapeytoia* Hou, Bergström, and Ahlberg, 1995; *Perspicaris* Briggs, 1977; *Sanctacaris* Briggs and Collins, 1988; *Shankouia* Chen et al. in Waloszek et al., 2005; *Sidneyia* Walcott, 1911; *Sklerolibyon* Aria et al., 2020; *Triops* Schrank, 1803; *Waptia* Walcott, 1912; *Weinbergina* Richter and Richter, 1929; *Xandarella* Hou, Ramsköld, and Bergström, 1991; and *Yohoia* Walcott, 1912.

rod-like biramous trunk limbs (i.e., Papilio-BiCar and Papilio-UniCar, each represented by the topology shown in Tree B).

In the examination of all five hypotheses, *Papiliomaris* n. gen. consistently clustered closely with two other taxa coded from the Waukesha biota (*Acheronauta* and *Parioscorpio*), despite having obvious morphological differences. All three taxa were coded by members of the same laboratory group, although we specifically attempted to reduce author- or lab-specific coding bias by referring to taxa with similar features by Aria (2020) and observing how they were coded to ensure correct and consistent interpretations of character descriptions, as well as to determine any character dependencies (i.e., identifying which subsequent characters should be scored not applicable [NA] when an earlier character was coded as absent). But this relationship remained despite these efforts. This

https://doi.org/10.1017/jpa.2025.10102 Published online by Cambridge University Press

observation raises a pertinent question about the potential susceptibility of the arthropods' character matrices to author-specific coding biases, thereby carrying significant implications on final interpretations.

An aspect of the character matrix used in this study that contributes to this consideration is the pronounced emphasis on features that are rarely or never preserved in some fossil taxa, often specific to more derived clades. These group-specific characters carry equal weight compared to other characters in the matrix, potentially diluting the impact of more generalized features and placing a higher emphasis on specific crownward groups. Although the inclusion of these characters is necessary for the separation of better-understood clades, it also, unfortunately, leads to the aggregation of disparate fossil groups that outwardly appear to cluster based on the absence of these specific characters rather than similarities among those taxa.

The obvious solution to an abundance of characters that are too derived to be applicable to *Papiliomaris* n. gen. would be to use a clade-specific tree, or one that concentrates solely on basal taxa. But the dilemma confronting *Papiliomaris* n. gen. is that it would not be known in which derived clade it should be coded. *Papiliomaris* n. gen. does not contain obvious synapomorphies of Crustacea, Myriapoda, or Chelicerata, but it also shows a sufficient derivation of traits, especially of the limb number and structure, to suggest that a basal taxon cladogram would also be insufficient. This raises an additional possibility that the clustering of *Captopodus*, *Acheronauta*, *Parioscorpio*, and now *Papiliomaris* n. gen. at the base of the Mandibulate branch is real, and that these are 'intermediate' stem taxa, neither basal nor derived with respect to the total-arthropod tree.

These taxa could represent a distinct phase in arthropod evolution, historically less understood due to the scarcity of middle Paleozoic deposits preserving soft tissues in arthropods. We argue that it is no coincidence that the individual taxa nearest to the 'Waukesha biota' on Tree A and Tree B are from the Silurian Herefordshire Lagerstätte (*Tanazios dokeron* Siveter et al., 2007; *Cascolus ravitis* Siveter et al., 2017) and the Devonian Hunsrück Slate (*Captopodus poschmanni* Kühl and Rust, 2012).

A final consideration for the clustering of these taxa is a taphonomic one. Specific formations and facies within formation can have distinct taphonomic tendencies (e.g., Liu et al., 2018; Aria et al., 2023), so that some morphological features are usually preserved better than others, are preserved in a distinct manner, or not be preserved at all (e.g. Anderson and Smith, 2017). These could potentially lead to clusters of characters specific to certain tissues or morphological features being more completely coded, or not coded at all, on a lagerstätte-by-lagerstätte basis. The small size of many mid-Paleozoic lagerstätten (e.g. Kluessendorf, 1994), in particular, makes it less likely to capture a spectrum of taphonomic variability within a taxon. To illustrate, just like *Parioscorpio*, *Acheronauta*, and *Papiliomaris* n. gen., *Tanazios* Siveter et al., 2007 and *Cascolus* Siveter et al., 2017 are sister taxa and are both from the Herefordshire lagerstätte (and, indeed, were described by many of the same authors), as are sister taxa *Offacolus* Orr et al., 2000 and *Dibasterium* Briggs et al., 2012 (Orr et al., 2000; Briggs et al., 2012), within the stem chelicerates (Fig. 6).

Although attempting to understand the relationships among stem arthropods like *Papiliomaris* n. gen. is unquestionably a formidable task, the clustering of fossil taxa, influenced by limitations in information derived from fossil records and temporospatial considerations, underscores the need to introduce additional taxa from the middle Paleozoic. In fact, intermediary taxa like *Papiliomaris* n. gen., *Acheronauta*, *Parioscorpio*, and others, which defy easy classification within established groups, possess the potential to offer critical insights when deciphering the historical relationships between known clades. Thus, we advocate for continued investment in adding taxa like *Papiliomaris* n. gen. and the other Waukesha oddities to phylogenetic analyses of this nature. Eventually, we anticipate that the apparent closeness of the relationships between taxa like *Acheronauta*, *Parioscorpio*, and *Papiliomaris* n. gen. will be seen to be an illusion cast by a lack of data for taxa in this 'grade' of evolution to crown-group Crustacea and Myriapoda.

Taphonomy. *Papiliomaris kluessendorfae* n. gen. n. sp. shows similar preservation to previously reported members of the Waukesha Biota. Samples consist of mixtures of phosphatization with francolite (a fluorapatite-rich carbonate; Fig. 7.3, 7.4), moldic preservation, and carbonaceous compression, which are variably expressed in individual specimens (Kluessendorf, 1990; Wendruff et al., 2020a; Anderson et al., 2021; Pulsipher et al., 2022). Of the three taphonomic modes observed, phosphatization in francolite best conserved morphological details in our samples. Some fossils exhibit thick layers of francolite, which helped to better maintain three-dimensionality; the francolite appears in white or tan layers and is most often associated with head appendages three through five (Fig. 7.1, 7.3). Although there are fewer examples of francolite preserving trunk morphology (Fig. 7.1, 7.4), it appears to be thickest in the trunks of specimens in which the limbs are poorly preserved (Fig. 5.1, 5.4–5.8). Within the head, francolite also appears to be thicker in association with the axial regions (e.g. Figs. 4.6, 5.5, 5.6). Such thickenings could represent phosphatized visceral mass or muscle tissue, but textures confirming this interpretation have thus far remained elusive. The observed moldic preservation with little to no phosphatization is an inferred result of splitting fossil materials that experienced francolite replacement, in which the counterpart that does not retain very much francolite appears as a subdued or compressed three-dimensional mold (Fig. 5.5). Lastly, most samples contain a minor carbon film that demarcates the fossil outline, usually visible as a darkened matrix extending beyond any francolite replacement (e.g., Fig. 4.1–4.4). In some samples, simple structures are recognizable in the carbon-rich imprint, e.g., the pleurae in sample UWGM 2862 (Fig. 5.9), but this is uncommon.

The abundance of francolite within these fossils relates to the anoxic traps formed on the karstified surface of the Manistique Formation paleoscarp during the deposition of the Brandon Bridge Formation (Supplemental Fig. 1; Kluessendorf, 1990). This depositional environment favors the dissolution and replacement of carbonate materials (Mikulic et al., 1985a; Kluessendorf, 1990; Jones et al., 2015a; Jones and Tashman, 2016; Miller et al., 2022). We propose that, during the burial and decay of these organisms, any carbonate- or phosphate-bearing shells in the fauna, e.g., conulariids (e.g., Miller et al., 2022) or lightly mineralized arthropod carapaces, would dissolve in the acidic conditions of the sediment traps. The lowered pH would be produced during the course of microbial decay of molts and carcasses washed into the traps by the release of organic acids, H^+, and the formation of carbonic acid from carbon dioxide (Fenchel and Finlay, 1995; Atlas and Bartha, 1998; Wilson and Butterfield, 2014; Naimark et al., 2016). The confined nature of the traps ensured that they would have little circulation to disperse accumulated acidity (Kluessendorf, 1990). Those dissolved carbonates and phosphates would then subsequently reprecipitate around the labile tissues and other delicate

https://doi.org/10.1017/jpa.2025.10102 Published online by Cambridge University Press

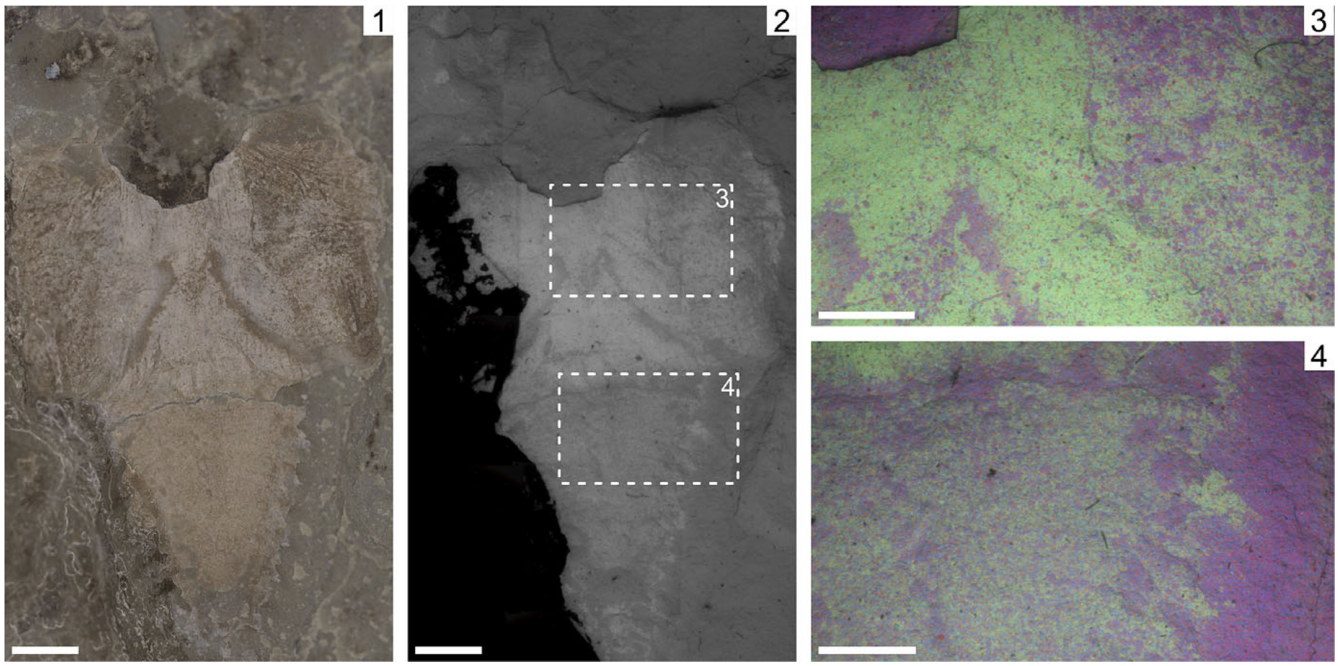

Figure 7. SEM and EDS analyses of holotype specimen, UWGM 2655. (**1, 2**) Z-stacked reflected light photograph, corresponding to same view in (**2**). (**2**) SEM-ATLAS backscattered electron mosaic image; labeled boxes indicate areas shown in (**3**) and (**4**). Dark/black region to lower left is epoxy or stabilization glue that provides structural integrity to the thin and friable rock sample hosting this fossil. (**3, 4**) EDS elemental mapping of regions highlighted in (**2**) showing, respectively, more robust francolite on the head appendages and lighter/thinner mineralization of the trunk. Seafoam green colorization represents the overlap of calcium and phosphorus maps, corresponding to francolite mineralization. Purple colorization represents the aluminosilicate-rich host lithology. Scale bars = 2 mm (**1, 2**); 1 mm (**3, 4**).

features of the abundant arthropods, e.g., the finely preserved head limbs. These features would generally not be preserved in other environments where rapid, oxic decay is favored, and biomineralized material would largely remain intact.

This proposed taphonomic history is consistent with the samples presented in this study, as well as recently published observations of other arthropods from the Waukesha biota (e.g., Anderson et al., 2021; Pulsipher et al., 2022). Specimens of *Papiliomaris kluessendorfae* n. gen. n. sp. oriented with the carapace pressed directly on top of the head appendages can preserve much of the detailed limb structures, including the filamentous setae. In this burial orientation, the carapace probably also helped to create a microenvironment trapping decay products underneath the valves, which in turn better enabled phosphatization (Briggs and Kear. 1993, 1994; Briggs and Wilby, 1996; Wilby and Briggs, 1997). In contrast, specimens with a lifted carapace preserved head structures poorly (Fig. 5.1–5.4). Most commonly, in this situation, the head limbs decayed away, leaving only the molds of head segments preserved, if any evidence at all. This led us to conclude that the head limbs and their delicate rows of setae are generally only preservable when overlain by the carapace.

We do not know if the carapace was biomineralized in any way. Variability in the structure of the ribbing on the carapace could provide some clues, and the ribs do seem to be distinct from the often similar-sized limb setae, because the former can cross the entirety of the carapace. Nonetheless, it is not clear if these ribs are morphological features of the carapace or instead taphonomic artifacts. Even if authentic, their variability in spacing and directionality (Figs. 4.2, 4.3, 4.6–4.8, 5.5–5.8), and occasional wrinkled appearance (Fig. 5.2, 5.3) could be consistent with taphonomic modification of both biomineralized and purely organic structures. If biomineralized, demineralization and reprecipitation onto the delicate features below before they could decay might also have enhanced preservation.

Additionally, structures not located underneath the cephalic carapace are infrequently or poorly preserved in the samples, as seen in the first pair of antennae and the trunk across most samples. Notably, the second pair of antennae seems only to be preserved under the carapace (Figs. 3.3, 4.2, 4.3). This phenomenon is also likely the cause of the poor preservation of the trunk limbs. Without the microenvironment provided by an overlying carapace (and perhaps its phosphate and/or carbonate), all that is left after decay is the gross morphology of the trunk segments due to the recalcitrant nature of the chitin (Figs. 2.1, 2.2, 4.1, 4.4, 5.4, 5.9). The apparent preservation of detailed, three-dimensional limbs without a carapace in UWGM 2654 (Fig. 3.6–3.9) might be seen as the exception that proves the rule. Even the trunk is preserved in relatively three-dimensional phosphate that hints at the retention of internal or delicate external morphologies in this sample. This is the only specimen we have observed that exhibits this level of preservation without a carapace and could simply represent a glut of local phosphate that was available in an unusual circumstance. Thus, both the morphology of *Papiliomaris kluessendorfae* n. gen. n. sp. and the suite of conditions present in the Waukesha depositional environment were equally important in the preservation of these fossils.

Conclusions

In this study, we formally described and conducted a phylogenetic analysis on a previously unnamed taxon, the butterfly animal *Papiliomaris kluessendorfae* n. gen. n. sp. This Silurian-aged arthropod has a distinctive morphology characterized by elongate setae-bearing head limbs and a compact trunk. The orientation of the carapace

https://doi.org/10.1017/jpa.2025.10102 Published online by Cambridge University Press

directly controls the quality of preservation of the head limbs. Features covered by the carapace during burial show superior preservation, whereas those exposed are rarely preserved or show significant degradation. Like other recently investigated arthropods from the Waukesha biota (Anderson et al., 2021; Pulsipher et al., 2022), most of the morphological features of *P. kluessendorfae* n. gen. n. sp. are preserved in francolite, the constituents of which can be sourced in part from the dissolution of shelly animals in the fauna (e.g., Miller et al., 2022), or locally from the carapace (if lightly mineralized) during decay.

In the phylogenetic analysis, *Papiliomaris kluessendorfae* n. gen. n. sp. closely aligned with two others previously described from the Waukesha Lagerstätte: *Parioscorpio* and *Acheronauta*, as sister to Mandibulata. The juxtaposition of these fossil taxa within our phylogenetic analyses prompts not only a closer examination of other arthropod taxa in the Waukesha biota but also necessitates the continued addition of other problematic taxa within this temporal window, e.g., those from the Herefordshire and Eramosa lagerstätten. This holistic approach is crucial for enhancing our understanding of this specific interval within arthropod evolution. The highly dynamic and flexible body plan of arthropods can often lead to incomplete or inaccurate phylogenies when relying on only data of extant taxa. Phylogenetic studies that attempt to categorize arthropods that do not obviously belong to any well-established clades necessitate a total-group approach. Yet, the characters within such an analysis cannot contain too many crown-group specific characters if they are to be useful in resolving the placement of stemward taxa. The incorporation of genomics along with extant and extinct morphologies should help to provide a more complete appreciation of the intricate relationships of arthropods, but this underscores the need for additional comprehensive taxonomic studies on unique taxa that do not neatly fit within our current understanding of the phylum.

Acknowledgments. The authors thank the Waukesha Lime and Stone Company and Franklin Aggregate Inc. quarries in Waukesha, Wisconsin, for providing tours to see the Brandon Bridge Formation; C. Eaton at the University of Wisconsin–Madison Geology Museum for accessing and loaning specimens; and A. Russo for Keyence imaging of the specimens. Authors Anderson and Rosbach contributed equally to this work.

Competing interests. The authors declare no competing interests.

Data availability statement. Supplemental data are available from the Dryad Digital Repository: https://doi.org/10.5061/dryad.573n5tbn1 and Zenodo Digital Repository: https://doi.org/10.5281/zenodo.16996331.

References

Abushik, A.F., 2015, Ostracods (Crustacea): some problems of systematics: *Paleontological Journal*, **v. 49**, p. 485–495, https://doi.org/10.1134/S0031030115050020

Anderson, E.P., and Smith, D.M., 2017, The same picture through different lenses: quantifying the effects of two preservation pathways on Green River Formation insects: *Paleobiology*, **v. 43**, p. 224–247, https://doi.org/10.1017/pab.2016.29

Anderson, E.P., Schiffbauer, J.D., Jacquet, D.M., Lamsdell, J.C., Kluessendorf, J., and Mikulic, D.G., 2021, Stranger than a scorpion: a reassessment of *Parioscorpio venator*, a problematic arthropod from the Llandoverian Waukesha Lagerstätte: *Palaeontology*, **v. 64**, p. 429–474, https://doi.org/10.1111/pala.12534

Aria, C., 2020, Macroevolutionary patterns of body plan canalization in euarthropods: *Paleobiology*, **v. 46**, p. 569–593, https://doi.org/10.1017/pab.2020.36

Aria, C., and Caron, J.-B., 2017, Burgess Shale fossils illustrate the origin of the mandibulate body plan: *Nature*, v. **545**, p. 89–92, https://doi.org/10.1038/nature22080

Aria, C., Zhao, F., and Zhu, M., 2021, Fuxianhuiids are mandibulates and share affinities with total-group Myriapoda: *Journal of the Geological Society*, **v. 178**, n. jgs2020-246, https://doi.org/10.1144/jgs2020-246

Aria, C., Vannier, J., Park, T.-Y.S., and Gaines, R.R., 2023, Interpreting fossilized nervous tissues: *Bioessays*, **v. 45**, n. e2200167, https://doi.org/10.1002/bies.202200167

Atlas, R.M., and Bartha, R., 1998, Biogeochemical cycling: nitrogen, sulfur, phosphorous, iron, and other elements, *in* Atlas, R.M., and Bartha, R., *Microbial Ecology: Fundamentals and Applications* (fourth edition): Menlo Park, California, Benjamin/Cummings Publishing Company, p. 414–459.

Berdan, J.M., 1984, Leperditicopid ostracodes from Ordovician rocks of Kentucky and nearby states and characteristic features of the order Leperditicopida: *Geological Survey Professional Paper*, v. 1066-J, **40** p., 11 pls.

Braddy, S.J., and Dunlop, J.A., 2021, A sting in the tale of *Parioscorpio venator* from the Silurian of Wisconsin: is it a cheloniellid arthropod?: *Lethaia*, **v. 54**, p. 603–609, https://doi.org/10.1111/let.12457

Briggs, D.E.G., 1976, The arthropod *Branchiocaris* n. gen. Middle Cambrian, Burgess Shale, British Columbia: *Geological Survey of Canada Bulletin*, **v. 264**, p. 1–29.

Briggs, D.E.G., 1977, Bivalved arthropods from the Cambrian Burgess Shale of British Columbia: *Palaeontology*, **v. 20**, p. 595–621.

Briggs, D.E.G., and Collins, D., 1988, A middle Cambrian chelicerate from Mount Stephen, British Columbia: *Palaeontology*, **v. 31**, p. 779–798.

Briggs, D.E.G., and Kear, A.J., 1993, Fossilization of soft tissue in the laboratory: *Science*, **v. 259**, p. 1439–1442.

Briggs, D.E.G., and Kear, A.J., 1994, Decay and mineralization of shrimps: *PALAIOS*, **v. 9**, p. 431–456.

Briggs, D.E.G., and Wilby, P.R., 1996, The role of the calcium carbonate-calcium phosphate switch in the mineralization of soft-bodied fossils: *Journal of the Geological Society*, **v. 153**, p. 665–668.

Briggs, D.E.G., Erwin, D.H., and Collier, F.J., 1994, *Fossils of the Burgess Shale*: Washington D.C., Smithsonian Institution Press, 238 p.

Briggs, D.E.G., Sutton, M.D., Siveter, D.J., and Siveter, D.J., 2003, A new phyllocarid (Crustacea: Malacostraca) from the Silurian Fossil-Lagerstätte of Herefordshire, UK: Proceedings of the Royal Society B: *Biological Sciences*, **v. 271**, p. 131–138,

Briggs, D.E.G., Siveter, D.J., Siveter, D.J., Sutton, M.D., Garwood, R.J., and Legg, D., 2012, Silurian horseshoe crab illuminates the evolution of arthropod limbs: *Proceedings of the National Academy of Sciences*, **v. 109**, p. 15702–15705, https://doi.org/10.1073/pnas.1205875109

Briggs, D.E.G., Siveter, D.J., Siveter, D.J., Sutton, M.D., and Legg, D., 2016, Tiny individuals attached to a new Silurian arthropod suggest a unique mode of brood care: *Proceedings of the National Academy of Sciences of the United States of America*, **v. 113**, p. 4410–4415, https://doi.org/10.1073/pnas.1600489113

Brongniart, A., 1822, Les trilobites, *in* Brongniart, A., and Desmarest, A.G., 1822, *Histoire Naturelle des Crustacés Fossiles, sous les Rapports Zoologiques et Géologiques*: Paris, F.G. Levrault, p. 1–65.

Budd, G.E., 2008, The earliest fossil record of the animals and its significance: Philosophical Transactions of the Royal Society B: *Biological Sciences*, **v. 363**, p. 1425–1434, https://doi.org/10.1098/rstb.2007.2232

Caster, K.E., and Brooks, H.K., 1956, New fossils from the Canadian Chazan (Ordovician) hiatus in Tennessee: *Bulletins of American Palaeontology*, **v. 36**, p. 157–199.

Chen, J., Waloszek, D., and Maas, A., 2004, A new 'great-appendage' arthropod from the lower Cambrian of China and homology of chelicerate chelicerae and raptorial antero-ventral appendages: *Lethaia*, **v. 37**, p. 3–20, https://doi.org/10.1080/00241160410004764

Collette, J.H., and Hagadorn, J.W., 2010, Early evolution of phyllocarid arthropods: phylogeny and systematics of Cambrian-Devonian archaeostracans: *Journal of Paleontology*, **v. 84**, p. 795–820, https://doi.org/10.1666/09-092.1

Edgecombe, G.D., 2010, Arthropod phylogeny: an overview from the perspectives of morphology, molecular data and the fossil record: *Arthropod Structure & Development*, **v. 39**, p. 74–87, https://doi.org/10.1016/j.asd.2009.10.002

Farrell, Ú.C., Briggs, D.E.G., and Gaines, R.R., 2011, Paleoecology of the olenid trilobite *Triarthrus*: new evidence from Beecher's Trilobite Bed and other sites of pyritization: *PALAIOS*, **v. 26**, p. 730–742, https://doi.org/10.2110/palo.2011.p11-050r

Fenchel, T., and Finlay, B.J., 1995, *Ecology and Evolution in Anoxic Worlds*: New York, Oxford University Press, 276 p.

Gabbott, S.E., Browning, C., Theron, J.N., and Whittle, R.J., 2017, The late Ordovician Soom Shale Lagerstätte: an extraordinary post-glacial fossil and sedimentary record: *Journal of the Geological Society*, **v. 174**, p. 1–9, https://doi.org/10.1144/jgs2016-076

Gass, K.C., and Braddy, S.J., 2023, The Waukesha Biota: a wonderful window into early Silurian life: *Geology Today*, **v. 39**, p. 169–176, https://doi.org/10.1111/gto.12447

Giribet, G., and Edgecombe, G.D., 2019, The phylogeny and evolutionary history of arthropods: *Current Biology*, **v. 29**, p. R592–R602, https://doi.org/10.1016/j.cub.2019.04.057

Gürich, G., 1932, "*Mimetaster*" n. gen. (Crustac., ord.?) anstatt *Mimaster*: *Paläontologische Zeitschrift*, **14**(1/2): 136.

Haug, C., Briggs, D.E.G., Mikulic, D.G., Kluessendorf, J., and Haug, J.T., 2014, The implications of a Silurian and other thylacocephalan crustaceans for the functional morphology and systematic affinities of the group: *BMC Evolutionary Biology*, **v. 14**, n. 159, https://doi.org/10.1186/s12862-014-0159-2

Hou, X.-G., 1987, *Three new large arthropods from lower Cambrian*, Chengjiang, eastern Yunnan: Acta Palaeontologica Sinica, **v. 26**, p. 272–285.

Hou, X.-G., 1999, New rare bivalved arthropods from the lower Cambrian Chengjiang fauna, Yunnan, *China: Journal of Paleontology*, **v. 73**, p. 102–116.

Hou, X., and Bergström, J., 1997, Arthropods of the lower Cambrian Chengjiang fauna, southwest China: *Fossils & Strata*, **v. 46**, p. 1–116.

Hou, X., Ramsköld, L., and Bergström, J., 1991, Composition and preservation of the Chengjiang fauna—lower Cambrian soft-bodied biota: *Zoologica Scripta*, **v. 20**, p. 395–411.

Hou, X.-G., Bergström, J., and Ahlberg, P., 1995, *Anomalocaris* and other large animals in the lower Cambrian Chengjiang fauna of Southwest China: *GFF*, v. **117**, p. 163–183.

Jaekel, O., 1921, Einen neuen Phyllocariden aus dem Unterdevon der Bundenbacher Dachschiefer: *Zeitschrift der Deutschen Geologischen Gesellschaft, Monatsberichte*, v. **72**, p. 290–292.

Jones, W.T., and Tashman, J.N., 2016, Exceptionally preserved *Dihogmochilina boothia* Copeland, 1970 (Ostracoda: Leperditicopida: Isochilinidae) from the Silurian Waukesha Biota, Wisconsin: autecological and phylogenetic implications, *in* Jones, W.T., *A taxonomic and morphologic assessment of some crustaceans and crustacean-like Problematica* [Ph.D. dissertation]: Kent, Ohio, Kent State University, p. 116–140.

Jones, W.T., Feldmann, R.M. and Schweitzer, C.E., 2015a, *Ceratiocaris* from the Silurian Waukesha Biota, Wisconsin: *Journal of Paleontology*, **v. 89**, p. 1007–1021, https://doi.org/10.1017/jpa.2016.22

Jones, W.T., Feldmann, R.M., Schweitzer, C.E., and Wendruff, A.J., 2015b, The first post-Cambrian marrellomorph arthropod from North America: *Abstracts with Programs, Geological Society of America Annual Meeting, Baltimore, Maryland*, **v. 47**, no. 7, p. 563.

Jordan, F.W.H., and von Meyer, H., 1854, Über die Crustaceen der Steinkohlenformation von Saarbrücken: *Palaeontographica*, **v. 4**, p. 1–15.

Kleffner, M.A., Norby, R.D., Kluessendorf, J., and Mikulic, D.G., 2018, Revised conodont biostratigraphy of lower Silurian strata of southeastern Wisconsin: Abstracts with Programs, *Geological Society of America, 52nd Annual North-central Section Meeting*, **v. 50**, no. 4, https://doi.org/10.1130/abs/2018NC-312921

Kluessendorf, J., 1990, *Depositional and taphonomic aspects of a Silurian (Brandon Bridge, Llandovery-Wenlock) fossil konservat lagerstätte from Waukesha, Wisconsin (U.S.A.), predictability of North American Silurian fossil konservat lagerstätten, and some insights into ichnofacies* [Ph.D. dissertation]: Urbana Champaign, University of Illinois, 115 p.

Kluessendorf, J., 1994, Predictability of Silurian Fossil-Konservat-Lagerstätten in North America: *Lethaia*, **v. 27**, p. 337–344.

Kluessendorf, J., and Mikulic, D.G., 1996, An early Silurian sequence boundary in Illinois and Wisconsin, *in* Witzke, B.J., Ludvigson, G.A., and Day, J., eds., *Paleozoic Sequence Stratigraphy: Views from the North American Craton*: Geological Society of America Special Paper 306, p. 177–185.

Kühl, G., and Rust, J., 2012, *Captopodus poschmanni* gen. et sp. nov. a new stem-group arthropod from the Lower Devonian Hunsrück Slate (Germany): *Arthropod Structure & Development*, **v. 41**, p. 609–622, https://doi.org/10.1016/j.asd.2012.06.004

Kühl, G., Briggs, D.E.G, and Rust, J., 2009, *A great-appendage arthropod with a radial mouth from the Lower Devonian Hunsrück Slate*, Germany: Science, **v. 323**, p. 771–773, https://doi.org/10.1126/science.1166586

Lamsdell, J.C., Briggs, D.E.G., Liu, H.P., Witzke, B.J., and McKay, R.M., 2015a, A new Ordovician arthropod from the Winneshiek Lagerstätte of Iowa (USA) reveals the ground plan of eurypterids and chasmataspidids: *Science of Nature*, **v. 102**, n. 63, https://doi.org/10.1007/s00114-015-1312-5

Lamsdell, J.C., Briggs, D.E.G., Liu, H.P., Witzke, B.J., and McKay, R.M., 2015b, The oldest described eurypterid: a giant Middle Ordovician (Darriwilian) megalograptid from the Winneshiek Lagerstätte of Iowa: *BMC Evolutionary Biology*, **v. 15**, n. 169, https://doi.org/10.1186/s12862-015-0443-9

Lankester, E.R., 1904, Memoirs: the structure and classification of the Arthropoda: *Quarterly Journal of Microscopical Science*, **v. 47**, p. 523–582.

Leach, W.E., 1819, Entomostraca, *in* Levrault, F., ed., *Dictionaire des Science Naturelles*, Volume **14**: Paris, Levrault & Schoell, p. 524–543.

Legg, D.A., 2015, The morphology and affinities of *Skania fragilis* (Arthropoda) from the middle Cambrian Burgess Shale: *Bulletin of Geosciences*, **v. 90**, p. 509–518, https://doi.org/10.3140/bull.geosci.1532

Legg, D.A., 2016, An acercostracan marrellomorph (Euarthropoda) from the Lower Ordovician of Morocco: *The Science of Nature*, **v. 103**, n. 21, https://doi.org/10.1007/s00114-016-1352-5

Legg, D., Sutton, M.D., Edgecombe, G.D., and Caron, J.-B., 2012, Cambrian bivalved arthropod reveals origin of arthrodization: *Proceedings of the Royal Society B: Biological Sciences*, **v. 279**, p. 4699–4704, https://doi.org/10.1098/rspb.2012.1958

Lehmann, W.M., 1956, *Vachonisia* nov. gen. anstatt Vachonia: *Paläontologische Zeitschrift*, v. **30**, p. 225.

Liu, J., Steiner, M., Dunlop, J.A., and Shu, D., 2018, Microbial decay analysis challenges interpretation of putative organ systems in Cambrian fuxianhuiids: *Proceedings of the Royal Society B: Biological Sciences*, **v. 285**, n. 20180051, https://doi.org/10.1098/rspb.2018.0051

Luo, H.L., Hu, S.X., Chen, L.Z., Zhang, S.S., and Tao, Y.H., 1999, *[Early Cambrian Chengjiang Fauna from Kunming Region, China]*: Yunnan, China, Yunnan Science and Technology Press, 129 p., 32 pls. (in Chinese with English summary).

Lustri, L., Gueriau, P., and Daley, A.C., 2024, Lower Ordovician synziphosurine reveals early euchelicerate diversity and evolution: *Nature Communications*, **v. 15**, n. 3808, https://doi.org/10.1038/s41467-024-48013-w

M'Coy, F., 1849, On the classification of some British fossil Crustacea, with notices of new forms in the University of Cambridge: *Annals and Magazine of Natural History*, **v. 2**, p. 412–414.

Meek, F.B., 1877, *United-States Geological Exploration of the Forthieth Parallel*: Volume **4**, Part 1, Palaeontology: Washington, D.C., United States Government Printing Office, 197 p.

Meyer, R.C., and Gunderson, G.O., 1986, Discovering a new Silurian soft-bodied fauna: *Waukesha County, Wisconsin: Rocks & Minerals*, **v. 61**, p. 310–319.

Mikulic, D.G., 1977, A preliminary revision of the Silurian stratigraphy of south-eastern Wisconsin with discussion of sites visited, *in* Nelson, K.G., ed., *The Geology of Southeastern Wisconsin*: 41st Annual Tri-State Geological Field Conference, Guidebook, p. A6–A34.

Mikulic, D.G., Briggs, D.E.G., and Kluessendorf, J., 1985a, A new exceptionally preserved biota from the lower Silurian of Wisconsin, U.S.A: *Philosophical Transactions of the Royal Society B: Biological Sciences*, **v. 311**, p. 75–85.

Mikulic, D.G., Briggs, D.E.G., and Kluessendorf, J., 1985b, A Silurian soft-bodied biota: *Science*, **v. 228**, p. 715–717.

Miller, A.A., Jacquet, S.M., Anderson, E.P., and Schiffbauer, J.D., 2022, *Conulariids from the Silurian (late Telychian)* Waukesha Lagerstätte, Wisconsin: Historical Biology, **v. 34**, p. 2374–2394, https://doi.org/10.1080/08912963.2021.2017917

Miller, S.A., 1874, Genus *Megalograptus*: *Cincinnati Quarterly Journal of Science*, v. **1**, p. 343–346.

Moore, R.A., Briggs, D.E.G., Braddy, S.J., Anderson, L.I., Mikulic, D.G., and Kluessendorf, J., 2005, A new synziphosurine (Chelicerata: Xiphosura) from the late Llandovery (Silurian) Waukesha Lagerstätte, Wisconsin, USA:

https://doi.org/10.1017/jpa.2025.10102 Published online by Cambridge University Press

Journal of Paleontology, **v. 79**, p. 242–250, https://doi.org/10.1666/0022-3360(2005)079<0242:ANSCXF>2.0.CO;2

Moysiuk, J., Izquierdo-López, A., Kampouris, G.E., and Caron, J.B., 2022, A new marrellomorph arthropod from southern Ontario: a rare case of soft-tissue preservation on a Late Ordovician open marine shelf: *Journal of Paleontology*, **v. 96**, p. 859–874, https://doi.org/10.1017/jpa.2022.11

Müller, O.F., 1785, *Entomostraca seu Insecta Testacea, quae in Aquis Daniae et Norvegiae Reperit, Descripsit et Iconibus Illustravit*: Copenhagen, F.W. Thiele, 134 p.

Naimark, E., Kalinina, M., Shokurov, A., Boeva, N., Markov, A., and Zaytseva, L., 2016, Decaying in different clays: implications for soft-tissue preservation: *Palaeontology*, **v. 59**, p. 583–595, https://doi.org/10.1111/pala.12246

Novozhilov, N.I., 1960, Chlenistonogie, Trilobitoobraznye i Rakoobraznye, *in* Orlov, Yu. A., ed., *Osnovy Paleontologii*, Volume **8**: Moscow, Nedra, 199 p. (in Russian).

Orr, P.J., Siveter, D.J., Briggs, D.E.G., Siveter, D.J., and Sutton, M.D., 2000, A new arthropod from the Silurian Konservat-Lagerstätte of Herefordshire, UK: *Proceedings of the Royal Society of London B: Biological Sciences*, **v. 267**, p. 1497–1504, https://doi.org/10.1098/rspb.2000.1170

Ortega-Hernández, J., 2015, Lobopodians: *Current Biology*, **v. 25**, p. R873–R875.

Pulsipher, M.A., Anderson, E.P., Wright, L.S, Kluessendorf, J., Mikulic, D.G., and Schiffbauer, J.D., 2022, Description of *Acheronauta* gen. nov., a possible mandibulate from the Silurian Waukesha Lagerstätte, Wisconsin, USA: *Journal of Systematic Palaeontology*, **v. 20**, p. 1–24, https://doi.org/10.1080/14772019.2022.2109216

Rak, Š., Ortega-Hernández, J., and Legg, D.A., 2013, A revision of the Late Ordovician marrellomorph arthropod *Furca bohemica* from Czech Republic: *Acta Palaeontologica Polonica*, **v. 58**, p. 615–628, https://doi.org/10.4202/app.2011.0038

Rambaut, A., 2018, FigTree v. 1.4.4: http://tree.bio.ed.ac.uk/software/figtree (accessed September 2021).

Regier, J.C., Shultz, J.W., Zwick, A., Hussey, A., Ball, B., Wetzer, R., Martin, J. W., and Cunningham, C.W., 2010, Arthropod relationships revealed by phylogenomic analysis of nuclear protein coding sequences: *Nature*, **v. 463**, p. 1079–1083, https://doi.org/10.1038/nature08742

Richter, R., and Richter, E., 1929, *Weinbergina opitzi*, n.g., n.sp, ein Schwerttrttger (Merost., Xiphos,) aus dem Devon (Rheinland): *Senckenbergiana*, **v. 11**, p. 193–209.

Robison, R.A., and Babcock, L.E., 2011, Systematics, paleobiology, and taphonomy of some exceptionally preserved trilobites from Cambrian Lagerstätten of Utah: *Paleontological Contributions*, **v. 5**, p. 1−47, https://doi.org/10.17161/pc.1808.8543.

Ronquist, F., Teslenko, M., Van Der Mark, P., Ayres, D.L., Darling, A., et al., 2012, MrBayes 3.2: efficient bayesian phylogenetic inference and model choice across a large model space: *Systematic Biology*, **v. 61**, p. 539–542, https://doi.org/10.1093/sysbio/sys029

Rota-Stabelli, O., Campbell, L., Brinkmann, H., Edgecombe, G.D., Longhorn, S.J., Peterson K.J., Pisani, D., Philippe, H., and Telford, M.J., 2011, A congruent solution to arthropod phylogeny: phylogenomics, microRNAs and morphology support monophyletic Mandibulata: *Proceedings of the Royal Society B: Biological Sciences*, **v. 278**, p. 298–306, https://doi.org/10.1098/rspb.2010.0590

Scholtz, G., and Edgecombe, G.D., 2006, The evolution of arthropod heads: reconciling morphological, developmental and palaeontological evidence: *Development Genes and Evolution*, **v. 216**, p. 395–415, https://doi.org/10.1007/s00427-006-0085-4

Schrank, F.P., 1803, Flügellose Insekten, *in Favna Boica: durchgedachte Geschichte der in Baiern einheimischen und zahmen Thiere*, Volume **3**: Landshut, Germany, Philipp Krüll, p. 177–182.

Scott, H. W., 1961, Order Leperditicopida Scott, n. order, *in* Moore, R.C., ed., *Treatise on Invertebrate Paleontology, Part Q, Arthropoda*, Volume **3**: Boulder, Colorado, Geological Society of America (and University of Kansas Press), p. Q103–Q110.

Scourfield, D.J., 1926, On a new type of crustacean from the old red sandstone (Rhymie Chert Bed, Aberdeenshire)—*Lepidocaris rhyniensis*, gen. et sp. nov.: Philosophical Transactions of the Royal Society of London B: *Containing Papers of a Biological Character*, v. **214**, p. 153–187.

Serif Europe Ltd., 1987, Affinity Designer (version 1.9): https://affinity.serif.com/en-us/designer/ (accessed May 2025).

Siveter, D.J., Sutton, M.D., Briggs, D.E.G., and Siveter, D.J., 2007, A new probable stem lineage crustacean with three-dimensionally preserved soft parts from the Herefordshire (Silurian) Lagerstätte, *UK: Proceedings of the Royal Society B: Biological Sciences*, **v. 274**, p. 2099–2108, https://doi.org/10.1098/rspb.2007.0429

Siveter, D.J., Briggs, D.E.G., Siveter, D.J., Sutton, M.D., and Legg, D., 2017, A new crustacean from the Herefordshire (Silurian) Lagerstätte, UK, and its significance in malacostracan evolution: *Proceedings of the Royal Society B: Biological Sciences*, **v. 284**, n. 20170279, https://doi.org/10.1098/rspb.2017.0279

Siveter, D.J., Briggs, D.E., Siveter, D.J., and Sutton, M.D., 2020, The Herefordshire Lagerstätte: fleshing out Silurian marine life: *Journal of the Geological Society*, **v. 177**, p. 1–13, https://doi.org/10.1144/jgs2019-110

Stein, M., 2010, A new arthropod from the early Cambrian of North Greenland, with a 'great appendage'-like antennula: *Zoological Journal of the Linnean Society*, v. **158**, p. 477–500, https://doi.org/10.1111/j.1096-3642.2009.00562.x

Van Roy, P., and Briggs, D.E.G., 2011, A giant Ordovician anomalocaridid: *Nature*, v. **473**, p. 510–513, https://doi.org/10.1038/nature09920

Van Roy, P., Rak, Š., Budil, P., and Fatka, O., 2022, Redescription of the cheloniellid euarthropod *Triopus draboviensis* from the Upper Ordovician of Bohemia, with comments on the affinities of *Parioscorpio venator*: *Geological Magazine*, **v. 159**, p. 1471–1489, https://doi.org/10.1017/S0016756822000292

Vannier, J., Aria, C., Taylor, R.S., and Caron, J.B., 2018, *Waptia fieldensis* Walcott, a mandibulate arthropod from the middle Cambrian Burgess Shale: *Royal Society Open Science* **v. 5**, n. 172206, https://doi.org/10.1098/rsos.172206

Vannier, J., Wang, S.Q., and Coen, M., 2001, Leperditicopid arthropods (Ordovician-Late Devonian): functional morphology and ecological range: *Journal of Paleontology*, **v. 75**, p. 75–95, https://doi.org/10.1666/0022-3360(2001)075<0075:LAOLDF>2.0.CO;2

von Bitter, P.H., Purnell, M.A., Tetreault, D.K., and Stott, C.A., 2007, *Eramosa Lagerstätte—exceptionally preserved soft-bodied biotas with shallow-marine shelly and bioturbating organisms (Silurian*, Ontario, Canada): Geology, **v. 35**, p. 879–882, https://doi.org/10.1130/G23894A.1

Walcott, C.D., 1911, Cambrian Geology and Paleontology 2: No. 2, Middle Cambrian Merostomata, Cambrian Geology and Paleontology 2: *Smithsonian Miscellaneous Collections*, **v. 57**, p. 17–40.

Walcott, C.D., 1912, Middle Cambrian Branchiopoda, Malacostraca, Trilobita and Merostomata: Cambrian geology and paleontology II: *Smithsonian Miscellaneous Collections*, **v. 57**, p. 145–228.

Walcott, C.D., 1931, Addenda to descriptions of Burgess Shale fossils: *Smithsonian Miscellaneous Collections*, **v. 85**, p. 1–46.

Waloszek D., Chen, J.Y., Maas, A., and Wang, X.Q., 2005, Early Cambrian arthropods—new insights into arthropod head and structural evolution: *Arthropod Structure and Development*, **v. 34**, p. 189–205, https://doi.org/10.1016/j.asd.2005.01.005

Wendruff, A.J., Babcock, L.E., Kluessendorf, J., and Mikulic, D.G. 2020a, Paleobiology and taphonomy of exceptionally preserved organisms from the Waukesha Biota (Silurian), Wisconsin, USA: *Palaeogeography, Palaeoclimatology, Palaeoecology*, **v. 546**, n. 109631, https://doi.org/10.1016/j.palaeo.2020.109631

Wendruff, A.J., Babcock, L.E., Wirkner, C.S., Kluessendorf, J. and Mikulic, D.G. 2020b, A Silurian ancestral scorpion with fossilised internal anatomy illustrating a pathway to arachnid terrestrialisation: *Scientific Reports*, **v. 10**, n. 14, https://doi.org/10.1038/s41598-019-56010-z

Westberg, M., 2019, *Enigmatic worm-like fossils from the Silurian Waukesha Lagerstätte*, Wisconsin, USA [B.Sc. thesis]: Lund, Sweden, Lund University, 26 p.

Wilby, P.R., and Briggs, D.E., 1997, Taxonomic trends in the resolution of detail preserved in fossil phosphatized soft tissues: *Geobios*, **v. 30**, p. 493–502.

Wilson, H.M., Briggs, D.E.G., Mikulic, D.G., and Kluessendorf, J., 2004, Affinities of the lower Silurian Waukesha 'myriapod': *Abstracts with Programs, Geological Society of America, Denver, Colorado*, **v. 36**, no. 5, p. 525.

Wilson, L.A., and Butterfield, N.J., 2014, Sediment effects on the preservation of Burgess Shale-type compression fossils: *PALAIOS*, **v. 29**, p. 145–154, https://doi.org/10.2110/palo.2013.075

Yang, J., Ortega-Hernández, J., Legg, D.A., Lan, T., Hou, J.B., and Zhang, X. G., 2018, Early Cambrian fuxianhuiids from China reveal origin of the

https://doi.org/10.1017/jpa.2025.10102 Published online by Cambridge University Press

gnathobasic protopodite in euarthropods: *Nature Communications*, **v. 9**, n. 470, https://doi.org/10.1038/s41467-017-02754-z

Zhai, D., **Ortega-Hernández, J.**, **Wolfe, J.M.**, **Hou, X.**, **Cao, C., and Liu, Y.**, 2019, Three-dimensionally preserved appendages in an early Cambrian stem-group Pancrustacean: *Current Biology*, **v. 29**, p. 171–177, https://doi.org/10.1016/j.cub.2018.11.060

Zhang, W.T., **Lu, Y.H.**, **Zhu, Z.L.**, **Qian, Y.Y.**, **Lin, H.L.**, **Zhou, Z.Y.**, **Zhang, S. G., and Yuan, J.L.**, 1980, *Cambrian Trilobite Faunas of Southwestern China*. Beijing, Science Press, 497 p.

Zhang, X., and Shu, D., 2005, A new arthropod from the Chengjiang Lagerstätte, early Cambrian, southern China: *Alcheringa: an Australasian Journal of Palaeontology*, **v. 29**, p. 185–194, https://doi.org/10.1080/03115510508619300

https://doi.org/10.1017/jpa.2025.10102 Published online by Cambridge University Press